CHAPTER 20

The Outer Stellar Layers

In the present chapter we shall discuss the actual physical boundary conditions which must be satisfied at a stellar surface (Sect. 20.1), and some of the conditions under which it is possible to approximate them by the simple boundary conditions of vanishing density and temperature (Sects. 20.2 and 20.4). Also, we shall discuss the boundary conditions that must be applied in the case of convective transfer in the outer stellar layers (Sects. 20.4 and 20.6). The structure of both radiative and convective envelopes* will be examined (Sects. 20.3 and 20.6), and regions on the Herzsprung-Russell (H-R) diagram where the envelopes are convective will be approximately determined (Sect. 20.5). The temperature distribution in stellar envelopes will be discussed in Sect. 20.7, and integrated adiabats in hydrogen and helium ionization zones (useful in discussions of convective envelopes) will be derived in Sect. 20.8. Unless we state otherwise, we shall assume that the regions of interest are of uniform composition and that no magnetic fields, which may affect convection, are present.

20.1 Photospheric Conditions

The *photosphere* may be considered, qualitatively, as the "visible surface" of a star; it is the layer from which the energy coming up from the deep interior is finally radiated away into space. It is obvious that the photosphere must have a finite temperature in order to maintain this steady outward flow of radiant energy.

For the purposes of work in stellar interiors it is usually sufficient to define the photosphere as the layer at which the *actual* temperature, T, is equal to the *effective* temperature, T_e:

$$T = T_p = T_e, \tag{20.1}$$

* By *stellar envelope* we mean those outermost stellar layers whose mass is large compared to the mass lying above the photosphere (*cf.* Sect. 20.1) but small compared to the mass of the whole star.

where the subscript p denotes the photospheric value of the appropriate quantity and T_e is defined by the relation

$$L = 4\pi R^2 \sigma T_e^4 . \tag{20.2}$$

Here L is the luminosity of the star, R is the radius of the photosphere (the "surface") of the star, and σ is the Stefan-Boltzmann constant. The justification for our use of (20.1) is that, according to the theory of stellar atmospheres, the radiation from an actual stellar atmosphere has approximately the same character as the radiation which would be emitted by a black surface whose temperature is equal to T_e. Equation (20.1) may be taken as the physical surface boundary condition for the temperature.

The physical surface boundary condition for the pressure (or density) follows from the requirement that the material above the photosphere shall have a finite optical thickness, *i.e.*, that, when the temperature T has fallen to the value T_e, the radiation shall be able to escape from the star. Before we can apply this requirement, we must know the temperature distribution in the atmosphere as a function of optical depth. This can be obtained to sufficient accuracy for work in stellar interiors by applying the so-called "Eddington approximation" to the equation

$$\frac{dp_r}{dr} = -\frac{\kappa\rho}{c}\frac{L_r}{4\pi r^2}, \tag{20.3}$$

where p_r is the frequency integrated radiation pressure, given in terms of the frequency integrated specific intensity I (assumed axially symmetric) by the relation (see Sect. 2.5)

$$p_r = \frac{2\pi}{c}\int_{-1}^{1} I(\mu)\mu^2 d\mu, \tag{20.4}$$

where we assume here and throughout this chapter that the refractive index is unity. Equation (20.3) is exact for an isotropic source function and for a *grey* atmosphere ($\kappa_\nu = \kappa = const.$, independent of frequency ν) in radiative equilibrium; it is also exact (under corresponding assumptions) if the atmosphere is non-grey and if κ is defined as the flux-weighted mean (*cf.* Chap. 8)

$$\kappa \equiv \frac{1}{F}\int_0^\infty \kappa_\nu F_\nu d\nu, \tag{20.5}$$

where F is the integrated net flux, related to I (again assumed axially symmetric) by the equation (see Sect. 2.2)

$$F=2\pi\int_{-1}^{1}I(\mu)\mu\mathrm{d}\mu. \tag{20.6}$$

Equation (20.3) is not exact if κ is interpreted as the *Rosseland* mean; however, the equation becomes increasingly more accurate with increasing depth since the flux-weighted mean then goes over into the Rosseland mean. In practical applications of (20.3) one nevertheless takes κ to be the Rosseland mean. We assume that $r\simeq R$, the stellar radius (so that we are neglecting curvature), and that $L_r = L$, the total luminosity, and assume that all energy is being carried by radiation. In this case we have $L_r/4\pi r^2 = F \simeq$ constant with depth throughout the thin, photospheric regions, whence (20.3) gives the result

$$p_r=\frac{F}{c}\tau+p_r(0), \tag{20.7}$$

where

$$\mathrm{d}\tau=-\kappa\rho\mathrm{d}r \tag{20.8}$$

is the element of (normal) optical depth and $p_r(0)$ denotes the surface value of the radiation pressure.

The Eddington approximation consists essentially in using, at *all* optical depths, the relation

$$p_r=\frac{1}{3}aT^4, \tag{20.9}$$

which is actually valid only for *large* optical depths (*cf.* Sect. 6.3). One also approximates the value of $p_r(0)$ by considering only outgoing radiation (that is, assuming no incident radiation on the top of the atmosphere) and assuming the specific intensity at the surface to be isotropic in all outward directions. We have

$$p_r(0)=\frac{2\pi}{c}\int_{0}^{1}I(0)\mu^2\mathrm{d}\mu=\frac{2\pi}{3c}I(0)$$

and

$$F=2\pi\int_{0}^{1}I(0)\mu\mathrm{d}\mu=\pi I(0),$$

which give

$$p_r(0)\simeq\frac{2}{3}\frac{F}{c}. \tag{20.10}$$

Using (20.9), with the relation $a = 4\sigma/c$, and (20.10) in (20.7), we have

$$\frac{4}{3}\frac{\sigma}{c}T^4=\frac{F}{c}\tau+\frac{2}{3}\frac{F}{c}$$

or

$$T^4=\frac{1}{2}\frac{F}{\sigma}\left(1+\frac{3}{2}\tau\right).$$

Writing $F = \sigma T_e^4$, we obtain, finally, the well-known "grey-atmosphere" approximation for the temperature distribution:

$$T^4=(1/2)T_e^4(1+(3/2)\tau)=T_0^4(1+(3/2)\tau), \tag{20.11}$$

where $T_0=(1/2^{1/4})T_e$ is the "boundary" temperature, *i.e.*, the value of T at $\tau = 0$ (where $\rho = 0$). Since $T = T_e$ defines the location of the photosphere, we have from (20.11) that

$$\tau_p=(2/3). \tag{20.12}$$

Thus the photosphere is located in our approximation at an optical depth of (2/3).

To determine the photospheric value of the pressure, P, we must make use of the equation of hydrostatic equilibrium:

$$\frac{dP}{dr}=-g_s\rho, \tag{20.13}$$

where $g_s(= GM/R^2)$ is the surface gravity, here regarded as constant throughout the thin photospheric regions, and P is the *total* pressure. Combining (20.8) and (20.13) gives

$$\frac{dP}{d\tau}=\frac{g_s}{\kappa} \tag{20.14}$$

or

$$P_p=g_s\int_0^{\tau_p}\frac{1}{\kappa}d\tau, \tag{20.15}$$

where we have taken $P = 0$ at $\tau = 0$, *i.e.*, we neglect radiation pressure.* While κ is actually a function of position above the photosphere, we can as a zeroth approximation evaluate κ *at* the photosphere and remove it from under the integral sign in (20.15). (We shall show in Sect. 20.4 that this approximation is accurate generally to within better than a factor of, say, 2 or 3). Thus

$$P_p\simeq/\frac{2}{3}\frac{g_s}{\kappa_p}. \tag{20.16}$$

* See footnote p. 591.

Equation (20.16) is then the approximate physical boundary condition which must be satisfied by the pressure at a stellar surface.*

An alternative interpretation of (20.16) is provided by using the expression for the pressure scale height,

$$H \equiv -\left(\frac{\mathrm{d} \ln P}{\mathrm{d}r}\right)^{-1} = \frac{P}{\rho g}, \tag{20.17}$$

for a star in hydrostatic equilibrium, in (20.16). Evaluating (20.17) at the photosphere and eliminating P_p between this equation and (20.16) we obtain

$$\kappa_p \rho_p H_s = (2/3) \tag{20.18}$$

as an equivalent expression of the condition implied by (20.12). Equation (20.18) can be interpreted as saying that the photosphere is the layer at which the ratio of the pressure scale height to the photon mean free path is approximately equal to unity. The photosphere is therefore quite literally the layer from which the photons can first escape directly from the star.

20.2 Solution of the Equations of Stellar Structure in the Outer Radiative Layers of a Star

For a number of reasons, one of which is to determine the effect on the interior solution of using $\rho_p = T_p = 0$ as the surface boundary conditions, we must examine the solution of the equilibrium equations in the outer stellar layers. This solution is greatly simplified by the fact that $M_r \simeq M$ in these regions, because of the relatively low densities existing in the outer parts of a star, *i.e.*, of the relatively great central mass concentration typical of stars. Also, we can set $L_r = L$, since the temperatures are too low here for thermonuclear reactions to contribute appreciably to the luminosity, and we neglect gravitational energy sources which can cause L_r to depend on r even outside the nuclear energy generating region.

* The value of P at $\tau = 0$ is actually $p_r(0)$, the radiation pressure at $\tau = 0$. Using the approximation (20.10) for $p_r(0)$ and the relation $L = 4\pi R^2 F$, it is easily seen that retaining the surface value $p_r(0)$ of P results in the presence of an additional factor on the right side of the final result (20.16) of

$$\left(1 + \frac{\kappa_p L}{4\pi c G M}\right) = \left(1 + 1.6 \times 10^{-4} \frac{\kappa_p L}{M}\right) \tag{20.16'}$$

if L and M are in solar units and κ_p is in cm^2/gm. This factor is nearly equal to unity for all stars whose (L/M) values do not greatly exceed the solar value, and we henceforth neglect this factor.

We shall assume here that radiative transfer obtains everywhere in the layers immediately below the photosphere, even if the material is convectively unstable (*cf.* Chap. 13); the case of convective transfer will be considered in Sect. 20.6. It is probably a good approximation to assume only radiative transfer in the outer layers of main sequence stars earlier than about A5 (say $T_e \geq 7500\,^\circ\mathrm{K}$) and perhaps of giants and supergiants earlier than, say, F5 and K0, respectively (*cf.* Sect. 20.5). Such stars may have convection zones, but they will probably be too thin and ineffective to play an important role in determining the structure of the stellar envelope or of the interior. We shall discuss the physical reasons for this difference in the role played by convection in the envelopes as compared to the role played by radiation in the envelope in Sect. 20.6.

The only equilibrium equations which are left to be integrated, then, are the hydrostatic equation and the equation of radiative transfer, which we write in the forms

$$\frac{1}{P}\frac{dP}{dr} = -\frac{g\rho}{P} = -G\frac{M_r}{r^2 P}\rho, \tag{20.19}$$

$$\frac{1}{T}\frac{dT}{dr} = -\frac{3\kappa\rho}{4ac}\frac{1}{T^4}\frac{L_r}{4\pi r^2}. \tag{20.20}$$

From these equations we obtain the expression for the radiative temperature gradient (with respect to pressure):

$$\nabla_r \equiv \left(\frac{d\ln T}{d\ln P}\right)_{\text{rad}} = \frac{1}{n_e+1}\,^* = \frac{3}{16\pi acG}\frac{L_r}{M_r}\frac{\kappa P}{T^4}$$

$$= \frac{3L}{16\pi acGM}\left(\frac{L_r}{L}\right)\left(\frac{M}{M_r}\right)\frac{\kappa P}{T^4}, \tag{20.21}$$

where n_e is the effective polytropic index (*cf.* (12.15)). Another useful form of (20.21) is obtained by writing $L = \pi acR^2 T_e^4$ (T_e = effective temperature) and g (local gravitational acceleration) $= GM_r/r^2$. We obtain

$$\nabla_r = \frac{3}{16}\frac{\kappa P}{T^4}\left(\frac{L_r}{L}\right)\left(\frac{R}{r}\right)^2\frac{T_e^4}{g}. \tag{20.21'}$$

Unless we specifically state otherwise, we shall in the remainder of this

* We actually have $\nabla_r = (n_e+1)^{-1}$ only in the case in which all the energy is being carried by radiation. In convectively unstable regions ∇_r is to be identified with the "fictitious radiative gradient" (*cf.* Sect. 14.1), *i.e.*, the true gradient which would obtain if all the energy were being carried by radiation. In the latter case $\nabla_r \neq (n_e+1)^{-1}$ in general.

chapter set $(L_r/L) \simeq 1$ and $(M_r/M) \simeq 1$ (as is appropriate for the outer stellar layers). In this case (20.21) becomes simply

$$\nabla_r = \frac{3L}{16\pi acGM}\frac{\kappa P}{T^4}. \tag{20.22}$$

(Note that $(L_r/L) \simeq 1$ and $(M_r/M) \simeq 1$ do *not* necessarily imply that $(r/R) \simeq 1$; thus (20.22) may be valid, under suitable circumstances, even if (r/R) is considerably less than unity; see Sect. 20.3). Finally, it is useful to note that the reciprocal of the constant factor in (20.22) may be written as

$$\frac{16\pi acGM}{3L} = \frac{16}{3}\frac{g_s}{T_e^4} = 1.292 \times 10^{-10}\frac{M}{L}\text{ c.g.s.}, \tag{20.23}$$

where $g_s (\equiv GM/R^2)$ is the surface gravity of the star and M and L are in solar units.

It is often possible to represent the opacity κ over the regions of interest by an interpolation formula of the form

$$\kappa = \kappa_0 \rho^n T^{-s} \tag{20.24a}$$

$$= \kappa_0' P^n T^{-n-s}, \tag{20.24b}$$

where κ_0, κ_0', n, and s are assumed to be constants in the relevant regions. In general, the n and s in (20.24b) are not the same as the n and s in (20.24a); however, for a perfect gas equation of state they are the same and, furthermore, in this case the relation between κ_0 and κ_0' is seen to be

$$\kappa_0' = \kappa_0 \left(\frac{\mu}{\mathscr{R}}\right)^n. \tag{20.25}$$

When (20.24b) is substituted into (20.22), the variables are separable and we have

$$P^n \mathrm{d}P = \frac{16\pi acGM}{3\kappa_0' L} T^{n+s+3} \mathrm{d}T.$$

Assuming that $P = P_0$ when $T = T_0$ (some arbitrary temperature), we have

$$P^{n+1} = \frac{n+1}{n+s+4} \cdot \frac{16\pi acGM}{3\kappa_0' L} \cdot T^{n+s+4}\left[\frac{1-(T_0/T)^{n+s+4}}{1-(P_0/P)^{n+1}}\right] \tag{20.26}$$

$$(n+s+4 \neq 0)$$

$$= (n+1) \cdot \frac{16\pi acGM}{3\kappa_0' L} \cdot \frac{\ln(T/T_0)}{1-(P_0/P)^{n+1}} \qquad (n+s+4=0), \tag{20.27}$$

where we have assumed (as we always shall unless otherwise indicated) that $n \neq -1$; in fact, we have $n \geq 0$ in practically all physically realistic cases of interest in the outer stellar layers. Solving directly for P in (20.26) and (20.27), we have also

$$\left(\frac{P}{P_0}\right)^{n+1} = 1 + \left(\frac{n+1}{n+s+4}\right)\frac{1}{\nabla_r^0}\left(\frac{T}{T_0}\right)^{n+s+4}\left[1-\left(\frac{T_0}{T}\right)^{n+s+4}\right] \qquad (n+s+4 \neq 0) \tag{20.27'}$$

$$= 1 + (n+1)\frac{1}{\nabla_r^0}\ln\left(\frac{T}{T_0}\right) \qquad (n+s+4=0), \tag{20.27''}$$

where

$$\nabla_r^0 \equiv \frac{3\kappa_0' L}{16\pi acGM}\frac{P_0^{n+1}}{T_0^{n+s+4}} \tag{20.27'''}$$

is the value of ∇_r corresponding to the values $P = P_0$, $T = T_0$. Using (20.24b), we may also write (20.26) and (20.27) in the forms

$$P = \frac{n+1}{n+s+4}\cdot\frac{16\pi acGM}{3\kappa L}\cdot T^4 \cdot \left[\frac{1-(T_0/T)^{n+s+4}}{1-(P_0/P)^{n+1}}\right] \qquad (n+s+4 \neq 0) \tag{20.28}$$

$$= (n+1)\cdot\frac{16\pi acGM}{3\kappa L}\cdot T^4 \cdot \frac{\ln(T/T_0)}{1-(P_0/P)^{n+1}} \qquad (n+s+4=0). \tag{20.29}$$

The corresponding expressions for ∇_r can be obtained by using the solutions (20.28) and (20.29) in (20.22):

$$\nabla_r = \frac{n+1}{n+s+4}\cdot\frac{1-(T_0/T)^{n+s+4}}{1-(P_0/P)^{n+1}} \qquad (n+s+4 \neq 0) \tag{20.30}$$

$$= (n+1)\cdot\frac{\ln(T/T_0)}{1-(P_0/P)^{n+1}} \qquad (n+s+4=0). \tag{20.31}$$

By using (20.27') and (20.27'') in (20.30) and (20.31), these last equations may also be written in the forms

$$\nabla_r = \frac{n+1}{n+s+4} + \left(\frac{T_0}{T}\right)^{n+s+4}\left[\nabla_r^0 - \frac{n+1}{n+s+4}\right] \qquad (n+s+4 \neq 0) \tag{20.30'}$$

$$= \nabla_r^0 + (n+1)\ln(T/T_0) \qquad (n+s+4=0), \tag{20.31'}$$

where ∇_r^0 is given by (20.27'''). We note that ∇_r as given by (20.30) and (20.31) or by (20.30') and (20.31') may exceed $\nabla_{ad} = (\Gamma_2 - 1)/\Gamma_2$, the adiabatic gradient (see (18.8') for a general formula for computing Γ_2). If it does, the

radiative gradient is convectively unstable (*cf.* Sect. 13.1), and the above results may have to be modified so as to include convective transfer; see Sect. 20.6.

It is to be noted that all the above solutions are valid *independently of the equation of state of the stellar material*, except insofar as the equation of state influences the form of the opacity law (20.24b). We shall discuss these solutions in the following sections.

20.3 Stellar Envelopes in Radiative Equilibrium

Here we consider stellar envelopes which may be regarded to good approximation as being everywhere in radiative equilibrium; hence (*cf.* Sects. 20.2 and 20.5) we are in effect concerned with rather hot stars ($T_e \gtrsim 7500\,°\mathrm{K}$, say, for the main sequence). We shall also restrict ourselves here to the regions of the envelope *below* the region of hydrogen ionization (say where $T \gtrsim 10^4\,°\mathrm{K}$). (The regions in and above the hydrogen ionization region will be considered in Sect. 20.4.) In such regions the electron density does not depend strongly on density and temperature (assuming a "normal" composition of predominantly hydrogen) and the opacity may be expected to behave in the same qualitative way as, for example, a Kramers opacity does. In other words, we are concerned here with regions of the star in which, say, the exponents n and s in the opacity law (*cf.* (20.24a,b)) are positive or zero (mathematically, we need only assume that $n+s > -4$ for the purposes of the present discussion). We shall also assume pure radiative transfer, even in regions which are convectively unstable (*cf.* Chap. 13). Modifications introduced by convection are discussed in Sect. 20.6.

We notice from the solutions (20.26)–(20.31′) of the radiative transfer equations in the envelope that for the case $n+s+4>0$, these solutions have an interesting property: as T rises above T_0 and P rises above P_0, the solutions become less and less sensitive to the values of T_0 and P_0 (T_0 and P_0 may be interpreted, for example, as photospheric values or as values at some point immediately below the region of hydrogen ionization). Moreover, the radiative gradient ∇_r and hence (assuming pure radiative transfer) the effective polytropic index n_e both approach constant values as one descends into the interior; *i.e.*, the envelope takes on a *polytropic* structure in the deeper layers (a polytropic structure is characterized by a constant value of the effective polytropic index). For sufficiently large values of T and P, in fact, all purely radiative solutions approach the one "radiative zero" solution (see Schwarzschild [Sc58b, Sect. 11]), which is characterized by $P_0 = 0$ and $T_0 = 0$ (vanishing surface pressure and temperature). Since the convergence of all purely radiative solutions to the one radiative zero

solution is extremely rapid in most cases (for example, $n+s+4 = 8.5$ for a Kramers opacity, $n = 1$, $s = 3.5$), it follows that in these cases the simple boundary conditions $P = T = 0$ at $r = R$ should provide excellent approximations to the correct ones. Hoyle and Schwarzschild [Ho55], however, have shown that these boundary conditions may not provide an adequate approximation to the actual situation in stars with very large radii and small masses (*i.e.*, giants of small mass). In these cases the photospheric pressure is reached, according to the radiative zero solution, so deep in the envelope that $1-r_p/R$ is not small compared to unity, r_p being the radial distance at which P (obtained from the radiative zero solution) is equal to P_p.

The radiative zero solution may be written in the form

$$P = KT^{n_e+1}, \tag{20.32}$$

where n_e has the constant value (see (20.21), (20.26), and (20.30′))

$$n_e=\frac{s+3}{n+1} \tag{20.33}$$

and where the constant K is given by the relations

$$K=\left[\frac{n+1}{n+s+4}\cdot\frac{16\pi acGM}{3\kappa_0' L}\right]^{1/(n+1)} \tag{20.34a}$$

$$=\left[\frac{n+1}{n+s+4}\cdot\frac{16\pi acGM}{3\kappa_0 L}\left(\frac{\mathscr{R}}{\mu}\right)^n\right]^{1/(n+1)}, \tag{20.34b}$$

where in (20.34b) we have assumed a perfect gas equation of state with constant mean molecular weight μ. For a Kramers opacity law ($n = 1$, $s = 3.5$) we have $n_e = 3.25$, and the radiative zero solution is

$$P=KT^{4.25},$$

where

$$K=\left[\frac{1}{4.25}\cdot\frac{16\pi acGM}{3\kappa_0 L}\frac{\mathscr{R}}{\mu}\right]^{1/2}.$$

Comparison of (20.30′) with the basic equation (20.22) shows that the quantity $\kappa P/T^4$ is constant in the radiative zero solution (which exists only for $n+s+4>0$). Thus, noting (20.24b), we see directly that $P \propto T^{n_e+1}$, where $n_e = (s+3)/(n+1)$, valid for the radiative zero solution.

Another interesting property of the radiative zero solution may be derived from the constancy of the quantity $\kappa P/T^4$. From this and the above we see that the variation of κ with depth in the envelope is given by the proportionality $\kappa \propto T^{3-n_e}$. Using (20.24b), (20.32), and (20.33), we have, more explicitly,

$$\kappa=\kappa_0' K^n T^{3-n_e}.$$

This shows that the opacity κ is strictly constant in the envelope (where the radiative zero solution is valid) if $n_e = 3$. Since realistic values of n and s usually lead to $n_e \simeq 3$, it follows that, typically, κ is a slowly varying function of depth in a radiative zero envelope.

Is the radiative zero solution stable against convection? As we have seen (*cf.* (13.13)), the condition for stability of the radiative gradient against convection in regions of uniform composition is that $n_e > 1/(\Gamma_2 - 1)$ or $\nabla_r < \nabla_{ad} \equiv (\Gamma_2 - 1)/\Gamma_2$, where (*cf.* (9.88) and (18.8′)) Γ_2 is the appropriate adiabatic exponent. But n_e is typically close to 3 (and ∇_r close to 0.25) for reasonable values of n and s. Moreover, outside of regions of partial ionization $\Gamma_2 = (5/3)$ and $\nabla_{ad} = 0.4$ for a non-relativistic, perfect monatomic gas in which radiation pressure is negligible. We conclude that the radiative zero solution is stable against convection under these conditions. In regions of partial ionization of an abundant element, however, this may not be true since Γ_2 approaches unity in such regions. Since the radiative zero solution is not generally valid in the regions of hydrogen ionization (to be discussed in the next section), it is normally only helium ionization that may produce convective instability in "radiative zero" envelopes (more specifically, *second* helium ionization since first helium ionization usually occurs very close to the hydrogen-ionization region).

Note (see (13.31)) that the specific entropy S decreases inward in convectively stable regions of a uniform composition radiative zero envelope in which no irreversible processes (such as nuclear reactions) are occurring.

The radiative zero solution (20.32) provides a remarkably good approximation to the structure of realistic stellar envelopes in radiative equilibrium (at least below the region of hydrogen ionization) computed by numerical integration of the structure equations on the basis of tabulated (*i.e.*, non-power law) opacities. Typically, for a reasonable opacity law the solutions (20.26)–(20.31′) will have converged to the radiative zero solution to good accuracy by the time T has reached, say, $2T_0$. Since T_0 is likely to be of the order of or less than 10^4 °K, levels deeper than, say, $(2-3) \times 10^4$ °K should normally be described adequately by the radiative zero solution (20.32).

We see, then, that the structure of stellar envelopes in radiative equilibrium (and also of the interior regions of the stars of which the envelopes form a part) are in most cases essentially independent of the surface boundary conditions, and the simple boundary conditions of vanishing surface pressure and temperature are usually adequate. In contrast, we shall see (*cf.* Sects. 20.5 and 20.6) that the internal structure of stars with *convective* envelopes is *critically* dependent on the surface boundary conditions. Hence the surface boundary conditions must be treated very carefully in such cases, which include most stars cooler than, say, 5000–7500 °K.

The solutions (20.26)–(20.31′) obtained in Sect. 20.2 and, more particularly, the polytropic radiative zero solution (20.32), may be expected to be good approximations to the structure of the envelope of a star whose outer layers are in radiative equilibrium and are chemically homogeneous, as long as $M_r \simeq M$ and $L_r \simeq L$. The first of these conditions will usually fail before the second will, because the energy sources (if nuclear) are usually strongly concentrated toward the center. This first condition ($M_r \simeq M$), however, in most cases is valid to fair accuracy throughout the outermost 30–50 per cent of the stellar radius, *i.e.*, possibly throughout the major portion of the stellar volume. For example, in the $n_e = 3$ polytrope (*cf.* Eddington [Ed26, Chap. 4]), which is a good rough approximation to the structure of most main sequence stars earlier than the late M's (which may be completely convective, *cf.* Limber [Li58]), we have the following tabulation:

$1-M_r/M$	r/R
0.045	0.58
.095	.51
.52	.29.

This table shows that in this case only about 10 per cent of the total mass lies in the outer half of the stellar radius. For this reason the simple solution (20.32) is extremely useful for a variety of purposes and should always be kept in mind for applications in approximate work.

It should be noted that the radiative gradient can be convectively unstable ($\nabla_r > \nabla_{ad} = (\Gamma_2 - 1)/\Gamma_2$) even in a stellar envelope having $n+s+4>0$ whose *radiative zero* solution is convectively stable ($(n+1)/(n+s+4) < \nabla_{ad}$). This would be the case, for example, if P_0 and T_0 were such that $\nabla_r^0 > \nabla_{ad}$ (see (20.27‴)). Convective transfer might therefore be important in the vicinity of the point (P_0, T_0) and the above solutions would no longer be applicable; the approach to the radiative zero solution might then be seriously impeded or prevented altogether (see Sect. 20.6). In general, the actual radiative gradient at a point characterized by a given temperature T will be *greater than* or *less than* the radiative zero value $(n+1)/(n+s+4)$ according as the pressure P at that point is *greater than* or *less than*, respectively, the corresponding radiative zero value $P_{R.Z.}$ (see (20.32)). That this last statement is true can be seen from the relation (*cf.* (20.22) and (20.32))

$$\nabla_r = \frac{n+1}{n+s+4}\left(\frac{P}{P_{R.Z.}}\right)^{n+1}. \tag{20.34′}$$

We may conclude that the larger is the pressure corresponding to a given temperature, the greater is ∇_r and hence the greater is the tendency for the

material to be convectively unstable. These considerations will be useful for the work in Sect. 20.6.

The distribution of temperature in the envelope will be considered in Sect. 20.7.

20.4 Radiative Transfer in the Photospheric and Sub-Photospheric Regions

In this section we are primarily interested in stars cooler than about 10^4 °K, *i.e.*, stars in which hydrogen is not fully ionized at the photosphere. In these stars we consider principally only the region between the photosphere and the level (at $T \sim 10^4$ °K) where hydrogen is appreciably (or nearly fully) ionized. In these regions most of the opacity arises from absorption by neutral hydrogen and by the negative hydrogen ion (H^-) (the latter source of absorption predominates over the former, generally, for $T \lesssim (6-7) \times 10^3$ °K). The opacity from both sources increases with increasing electron density (*cf.* Chap. 16) which, in turn, increases rapidly with increasing temperature in regions of partial ionization because of the nature of the Saha equation. It follows, then, that the opacity increases in these regions strongly with increasing temperature for given density or pressure, in marked contrast to the behavior of the opacity in regions below the hydrogen ionization region. The behavior of the solutions of the radiative transfer equations is therefore qualitatively different in these regions than in the deeper layers. Moreover, because of the proximity of these regions to the stellar surface, we cannot expect any sort of "radiative zero" solutions to be very useful; we must use the more general solutions in which the surface boundary conditions are "felt" by the regions farther in. It is for these reasons that we consider the superficial outermost layers separately from the deeper regions. We shall see that the solutions of the equations of radiative transfer are usually violently unstable against convection because of the rapid inward increase of the opacity. For stars with $T_e \lesssim 7300$ °K [Ba63] this convective instability leads to deep convective envelopes, which can be an important influence on the internal structure of such stars. In this section we shall ignore convection even in regions which are convectively unstable; effects of convection will modify the solutions which we shall obtain in some cases and these effects will be discussed in Sect. 20.6.

We shall assume here as in Sect. 20.3 that the opacity κ can be approximated by simple power law expressions such as those in (20.24), with n, s, κ_0, and κ_0' constant in the particular regions of interest (an alternative method of approximating the opacity in these outer regions has been used, for example, by Hoyle and Schwarzschild [Ho55]). It is clear from the above

discussion that we shall have to allow s to take on negative values in the regions of present interest. We also use surface gravity g_s and effective temperature T_e as parameters in place of M and L (see (20.23)). Finally, in the general solutions (20.26)–(20.31′) we shall interpret P_0 and T_0 as *boundary* values, where the "boundary" is defined by $\tau = 0$, see Sect. 20.1. Thus $P_0 = 0$ (we are therefore ignoring radiation pressure, see the footnote in Sect. 20.1) and T_0 (boundary temperature) $= T_e/2^{1/4}$ if the grey atmosphere temperature distribution formula (20.11) is used.

We write (20.26) for $P(T)$ in the form

$$P = P_p \cdot f(T, T_e),$$

where P_p is the *photospheric* pressure (where $T = T_e$) and $f(T, T_e)$ is a dimensionless function which takes into account the variation of pressure with depth; obviously, $f(T_e, T_e) = 1$. We have the following explicit expressions for P_p and $f(T, T_e)$, obtainable from (20.26), assuming that $T_0 = T_e/2^{1/4}$ and $P_0 = 0$ (*cf.* (20.11)):

$$P_p = \left\{ \frac{n+1}{n+s+4} \cdot \frac{16}{3} \frac{g_s}{\kappa_0'} \cdot T_e^{n+s} \cdot \left[1 - (1/2)^{\frac{n+s+4}{4}} \right] \right\}^{\frac{1}{n+1}}, \qquad (20.35a)$$

$$(n+s+4 \neq 0)$$

$$f(T, T_e) = \left\{ \frac{(T/T_e)^{n+s+4} - (1/2)^{\frac{n+s+4}{4}}}{1 - (1/2)^{\frac{n+s+4}{4}}} \right\}^{\frac{1}{n+1}}; \qquad (20.35b)$$

$$P_p = \left[(n+1) \cdot \frac{16}{3} \frac{g_s}{\kappa_0' T_e^4} \cdot \ln(2^{1/4}) \right]^{\frac{1}{n+1}}, \qquad (20.36a)$$

$$(n+s+4 = 0)$$

$$f(T, T_e) = \left[\frac{\ln(2^{1/4} T/T_e)}{\ln(2^{1/4})} \right]^{\frac{1}{n+1}}; \qquad (20.36b)$$

$$P_p = \left\{ \frac{n+1}{|n+s+4|} \cdot \frac{16}{3} \frac{g_s}{\kappa_0'} \cdot \frac{1}{T_e^{|n+s|}} \cdot \left[(2)^{\frac{|n+s+4|}{4}} - 1 \right] \right\}^{\frac{1}{n+1}}, \qquad (20.37a)$$

$$(n+s+4 < 0)$$

$$f(T, T_e) = \left[\frac{(2)^{\frac{|n+s+4|}{4}} - (T_e/T)^{|n+s+4|}}{(2)^{\frac{|n+s+4|}{4}} - 1} \right]^{\frac{1}{n+1}} \qquad (20.37b)$$

(κ_0' is defined in (20.24b)). Equation (20.37b) shows that in case $n+s+4<0$,

$$f(T, T_e) \to \left[\frac{(2)^{\frac{|n+s+4|}{4}}}{(2)^{\frac{|n+s+4|}{4}} - 1} \right]^{\frac{1}{n+1}} = \text{const.} \qquad (20.38)$$

in the limit as T increases beyond T_e; in other words, the pressure becomes independent of T when T becomes large compared to T_e and the pressure is then equal to a constant times P_p, which itself depends (for a given opacity law) only on g_s and T_e. For example, for $n = 1$ and $s = -9$ (a possible value in many cases), the limiting value of $f(T,T_e)$ is 1.41; *i.e.*, the pressure levels off with increasing temperature to about 1.4 times its photospheric value. Physically, a negative value of $(n+s+4)$ means a rapid inward increase in κ; in order for a given radiant flux to be transmitted, the temperature gradient (with respect to P, for example) must also increase inward. Eventually (if $n+s+4$ remains negative) the temperature gradient becomes so steep that P becomes insensitive to T in these regions.

This behavior of the temperature gradient is clearly revealed in the expression (see (20.30)) for the radiative gradient $\nabla_r = (\mathrm{d}\ln T/\mathrm{d}\ln P)_{\mathrm{rad}}$ (it is important to emphasize that in convectively unstable regions ∇_r really means the "fictitious radiative gradient" (see (14.12)), *i.e.*, the gradient that would obtain if all the energy were being carried by radiation). We may write (20.30) and (20.31) in the forms

$$\nabla_r = \frac{n+1}{n+s+4}\left[1-\left(\frac{T_e}{2^{1/4}T}\right)^{n+s+4}\right] \qquad (n+s+4\neq 0) \qquad (20.39)$$

$$= (n+1)\ln(2^{1/4}T/T_e) \qquad (n+s+4=0). \qquad (20.40)$$

If $n+s+4>0$, we see again that $\nabla_r \to (n+1)/(n+s+4)$ (the radiative zero solution) as T increases beyond T_e. If, on the other hand, $n+s+4<0$, we have

$$\nabla_r = \frac{n+1}{|n+s+4|}\left[\left(\frac{2^{1/4}T}{T_e}\right)^{|n+s+4|}-1\right], \qquad (20.41)$$

which shows that ∇_r increases with increasing depth in this case. It is clear that if $-(n+s+4)$ is large enough over a sufficiently large region, ∇_r could attain quite large values ($\gg 1$) and we would then expect violent convective instability. (We recall, *cf.* Sect. 13.1, that convective instability occurs in uniform composition regions whenever $\nabla_r > \nabla_{\mathrm{ad}}$, where $\nabla_{\mathrm{ad}} = (\Gamma_2-1)/\Gamma_2$. For $\Gamma_2 = (5/3)$ we have $\nabla_{\mathrm{ad}} = 0.4$. In the case of an abundant element undergoing ionization we have $\Gamma_2 \to 1$, whence $\nabla_{\mathrm{ad}} \to 0$. In this last case it is clear that ionization would further enhance any convective instability that may be present.)

We note that a density inversion can occur if κ increases inward sufficiently rapidly (*i.e.*, if $-(n+s+4)$ is large enough) and if the energy transfer is wholly radiative. Since in this case the pressure P becomes essentially

independent of T because of the steep temperature gradient, it follows that if $P \propto \rho T$ (perfect gas equation of state), for example, the density ρ must decrease with increasing depth in order that the product ρT remain approximately constant. It is easily seen that for a perfect gas equation of state with constant mean molecular weight μ, a density inversion occurs whenever $\nabla_r > 1$ (still assuming pure radiative transfer).

In Sect. 20.4a we shall consider the behavior of the solutions in and above the photosphere. In Sect. 20.4b we shall consider approximate power-law expressions for the opacity due to H and H^-, and in Sect. 20.4c we shall discuss some numerical results and conclusions regarding the outermost layers of cool stars.

20.4a Behavior of Solutions in Regions In and Above the Photosphere

We consider now the behavior of the solutions in the photospheric and superphotospheric regions. For this purpose it is instructive to use the approximate grey atmosphere temperature distribution (see (20.11)):

$$T^4 = (1/2)\, T_e^4 (1 + (3/2)\tau), \tag{20.42}$$

where τ denotes normal optical depth. We obtain from (20.39) and (20.40) the equations

$$\nabla_r = \frac{n+1}{n+s+4}\left[1 - \left(1+\frac{3}{2}\tau\right)^{-\frac{n+s+4}{4}}\right] \qquad (n+s+4 \neq 0) \tag{20.43}$$

$$= \frac{n+1}{4} \ln\left(1+\frac{3}{2}\tau\right) \qquad (n+s+4=0), \tag{20.44}$$

which show that $\nabla_r \to 0$ as $\tau \to 0$. Hence the (grey) atmosphere becomes isothermal at sufficiently small optical depths ($\tau \ll (2/3)$); in such regions P and ρ decrease outward exponentially: they vary approximately as $\exp[-(r-R)/H_s]$, where R is the photospheric radius (at $\tau = (2/3)$) and $H_s = \mathscr{R} T_e/\mu g_s$ (assuming a perfect gas equation of state) is the photospheric pressure scale height. We also see from (20.43) and (20.44) that the layers sufficiently far out in a stellar atmosphere are always in radiative equilibrium, at least within the framework of our simple physical picture.

At the photosphere ($\tau = (2/3)$) we have

$$\nabla_r^{(p)} = \frac{n+1}{n+s+4}\left[1 - \frac{1}{2}^{\frac{n+s+4}{4}}\right] \qquad (n+s+4 \neq 0) \tag{20.45}$$

$$= (1/4)(n+1)\ln 2 \qquad (n+s+4=0). \tag{20.46}$$

Also, since (see (20.22) and (20.23))

$$\frac{\kappa P}{g_s}=\frac{16}{3}\left(\frac{T}{T_e}\right)^4\cdot\nabla_r, \tag{20.47}$$

we have *at* the photosphere:

$$\frac{\kappa_p P_p}{g_s}=\frac{16}{3}\nabla_r^{(p)}=\frac{16}{3}\,\frac{n+1}{n+s+4}\left[1-\frac{1}{2}^{\frac{n+s+4}{4}}\right] \qquad (n+s+4\neq 0) \tag{20.48}$$

$$=(4/3)(n+1)\ln 2 \qquad (n+s+4=0). \tag{20.49}$$

We note that the values of ∇_r and $(\kappa P/g_s)$ at a given optical depth τ are independent of T_e; this is also obviously true for the photospheric values.

Table 20.1 gives values of $\nabla_r^{(p)}$ and $(\kappa_p P_p/g_s)$ for a grid of values of n and s.

Table 20.1

PHOTOSPHERIC VALUES OF ∇_r AND $(\kappa P/g_s)$

n	s	$n+s+4$	$\kappa_p P_p/g_s$	$\nabla_r^{(p)}$
0	0	+4	0.667 (= 2/3)	0.125
1	+3.5	+8.5	0.966	.181
1	+3	+8	1.00	.1875
1	+2	+7	1.07	.201
1	0	+5	1.14	.214
1	−2	+3	1.44	.270
1	−5	0	1.85	.347
1	−10	−5	2.93	.549*
1	−13	−8	4.00	.750*
1	−15	−10	4.94	.926*
0.5	+3	+7.5	0.78	.146
0.5	0	+4.5	0.96	.180
0.5	−3	+1.5	1.23	.239
0.5	−10	−5.5	2.32	.435*
0.5	−12.5	−8	3.00	.562*

* Values for which $\nabla_r^{(p)} > 0.4 = \nabla_{ad}$ for $\Gamma_2 = (5/3)$.

We see from Table 20.1 that the photosphere itself is stable against convection except in cases of extremely rapid inward increase of κ (*i.e.*, large values of $-(n+s+4)$). We also note that the values of $(\kappa_p P_p/g_s)$ do not differ from the value (2/3) appropriate for a constant opacity above the

photosphere by large factors (in all cases by less than a factor of 7 and in most cases by less than a factor of 2).

20.4b Interpolation Formulae for Opacity Due to H *and* H^-

Approximate power-law formulae for the opacity arising from neutral hydrogen (H) and the negative hydrogen ion (H^-) have been given by Hayashi, Hōshi, and Sugimoto [Ha62a]. Hayashi *et al.* start with the following expressions for the opacity due separately to H and H^-:

$$\kappa_{H^-} = 10^{-1.26} \cdot X(1-x)P_e(5040/T)^{4.3}\,\mathrm{cm}^2/\mathrm{gm}\,(2520 \lesssim T(^\circ\mathrm{K}) \lesssim 10{,}080), \tag{20.50}$$

$$\kappa_{H} = 10^{7.76}X(1-x) \cdot 10^{-12.14(5040/T)}\,\mathrm{cm}^2/\mathrm{gm}\,(6300 \lesssim T(^\circ\mathrm{K}) \lesssim 12{,}600), \tag{20.51}$$

where X is the relative mass abundance of hydrogen, x denotes the degree of ionization of hydrogen (the ratio of the number of hydrogen ions to the number of neutral and ionized hydrogen atoms), P_e denotes the electron pressure in c.g.s. units, and temperature T is in °K.

A general expression relating P_e to P_g, the gas pressure, was derived in Sect. 9.18 and is $P_e = [\bar{x}/(1+\bar{x})]P_g$, where $\bar{x}$ is the mean degree of ionization of the material. From this it is clear that the value of P_e depends, particularly at low temperatures, strongly on the source of the free electrons. For $T \lesssim 5000\,^\circ$K, most of the free electrons are supplied by single ionization of the metals (at these temperatures hydrogen is nearly completely neutral), whereas most free electrons are supplied by hydrogen ionization for $T \gtrsim 5000\,^\circ$K. It is therefore clear that the relation between P_g and P_e cannot depend very sensitively on the metal abundance for $T \gtrsim 5000\,^\circ$K. (5000 °K is approximately the temperature at which about as many electrons are supplied by the metals as by hydrogen ionization, *i.e.*, at which $x \sim A^{-1}$, where A is the "hydrogen/metal ratio"; A is of the order of 10^{+4} for Population I stars and perhaps one or two orders of magnitude larger for Population II stars.) For $2800 \leq T(^\circ\mathrm{K}) \leq 5040$ and $10^2 \leq P_g(\mathrm{dynes/cm}^2) \leq 10^{4.5}$, the electron pressure can be represented adequately, according to Hayashi *et al.* [Ha62a], for a composition close to a "Population I" composition ($X = 0.61$, $Y = 0.37$, and $Z = 0.02$, where X, Y, and Z are the relative mass abundances of hydrogen, helium, and heavy elements, respectively), by the formula

$$P_e = 10^{-30.16}\left(\frac{0.70}{X+0.25Y} \cdot \frac{Z}{0.02}P\right)^{0.74} T^{7.35}, \tag{20.52}$$

where c.g.s. units are used throughout, and where we neglect radiation pressure: $P \simeq P_g$.

On the basis of (20.52) Hayashi *et al.* derive the following approximate interpolation formulae for the total opacity due to both H and H^- absorption, for X, Y, and Z close to 0.61, 0.37, and 0.02, respectively:

$$\kappa = \kappa_0' P^{0.74} T^{3.05} \quad (T(^\circ\mathrm{K}) \lesssim 5040) \tag{20.53}$$

$$\kappa = \kappa_1' P^{0.74} T^{-0.74-s} \quad (5040 \lesssim T(^\circ\mathrm{K}) \lesssim 10{,}080), \tag{20.54}$$

where

$$\kappa_0' = 10^{-15.58} \frac{X}{0.61} \left(\frac{0.70}{X + 0.25Y} \cdot \frac{Z}{0.02} \right)^{0.74}, \tag{20.55}$$

$$\kappa_1' = \kappa_0' (5040)^{3.05+0.74+s}. \tag{20.56}$$

Comparison of (20.53) and (20.55) with (20.50) and (20.52) shows that for $T \lesssim 5040\,^\circ\mathrm{K}$, almost the entire contribution to the opacity is from the H^- ion. Values of $-(0.74+s)$ at a temperature of 5040 °K are given in Table 20.2

*Table 20.2**

VALUES OF EXPONENTS IN (20.54) AND (20.58)

$\log_{10} P$ (dynes/cm^2)	2		3		4		5	
	$-(n+s)$	$-s$	$-(n+s)$	$-s$	$-(n+s)$	$-s$	$-(n+s)$	$-s$
Pop. I ($n = 0.74$)	13.2	13.9	10.7	11.4	8.6	9.3	6.8	7.5
Pop. II ($n = 0.71$)	11.7	12.4	10.7	11.4	9.4	10.1	8.4	9.1

* Adapted from Hayashi *et al.* [Ha62a].

(Table 4.2 of Hayashi *et al.* [Ha62a]) as a function of $\log P$; this is the temperature at which (for this "Population I" composition) the switch-over from (20.53) to (20.54) is made. The value of κ_1' as given by (20.56) will insure continuity of κ at $T = 5040\,^\circ\mathrm{K}$. It is important to note that (20.53)–(20.56) are valid only for compositions close to the "Population I" composition. The switch-over from (20.53) to (20.54) presumably corresponds, physically, to a switch-over from electrons predominantly supplied by metals to electrons predominantly supplied by hydrogen. Since in the second case the electron pressure P_e and the degree of hydrogen ionization x cannot depend to any significant extent on metal abundance (or Z), κ_1' should be essentially independent of Z. A composition different from the above "Population I" composition would require a different "transition" temperature (say T_r), corresponding to the switch-over from (20.53) to (20.54). This transition temperature decreases with decreasing Z and, since $|n+s| > 3.05$, the factor

$T_r^{3.05+0.74+s}$ in (20.56) decreases with decreasing Z. If the calculation is done properly, κ_1' should turn out to be independent of Z.

For a "Population II" composition ($X = 0.90$, $Y = 0.10$, $Z = 0.001$), Hayashi *et al.* [Ha62a] give the following formulae:

$$\kappa = \kappa_0' P^{0.71} T^{3.86} \qquad (T(^\circ\mathrm{K}) \lesssim 4380), \tag{20.57}$$

$$\kappa = \kappa_1' P^{0.71} T^{-0.71-s} \quad (4380 \lesssim T(^\circ\mathrm{K}) \lesssim 10{,}080), \tag{20.58}$$

$$\kappa_0' = 10^{-19.14}, \kappa_1' = \kappa_0'(4380)^{3.86+0.71+s}, \tag{20.59}$$

where values of $0.71+s$ are also given in Table 20.2.

It should be mentioned that there will be a contribution to the opacity from molecular absorption for $T \lesssim 3600\,^\circ$K ([Ha62a, p. 78]; also Vardya [Va60a, 61, 64, 66]; Sommerville [So64]). For $T \gtrsim 2500\,^\circ$K, however, this effect is probably small [Ha62a, p.78] and is neglected in the above formulae.

These formulae and Table 20.2 show that for $T \lesssim 5000\,^\circ$K in stars composed predominantly of hydrogen, $s \simeq -4$ and $n+s+4 \simeq +1$; for $5000 \lesssim T(^\circ\mathrm{K}) \lesssim 10{,}000$, s ranges from about -13 to about -8 (representative value -9 or -10) and $n+s+4$ ranges from about -3 to about -9 (representative value -5 or -6).

20.4c Some Numerical Results and Conclusions

Tables 20.3 and 20.4 give some values of the radiative gradient ∇_r (see (20.39)) and the function $f(T, T_e)$ (see (20.35)) for several values of T and T_e on the basis of the foregoing formulae, assuming a "Population I" composition. (For $T \geq 5040\,^\circ$K, we have taken $s = -9.74$, giving $n+s+4$ the value

Table 20.3

VALUES OF ∇_r (*cf.* (20.39))

$T_e(10^3\,^\circ\mathrm{K})$	$T(10^3\,^\circ\mathrm{K})$					
	$T=T_e$	3.60	5.04	7.50	9.00	10.08
2.29	0.28	0.82	1.10	10.22	25.94	45.99
2.80	0.28	0.61	0.94	9.05	23.04	40.87
3.60	0.28	0.28	0.70	7.30	18.68	33.19
5.04	0.48		0.48	5.69	14.69	26.15
7.00	0.48			0.82	2.56	4.78
8.00	0.48				1.14	2.20
10.00	0.48					0.51

-5; for $T < 5040\,°\mathrm{K}$, we have used the value $s = -3.79$. Both ∇_r and $f(T, T_e)$ have been assumed continuous across the "transition" temperature 5040 °K; see (20.27″) and (20.30′).)

From these tables (or from equations (20.26)–(20.31′) and (20.35)–(20.41)) we can draw the following conclusions. First, we note that in all cases the value of the radiative gradient ∇_r increases steadily inward at least until the region (at $T \simeq 10{,}000\,°\mathrm{K}$) is reached where hydrogen is appreciably ionized; convective instability ($\nabla_r \geq 0.40$, say), in fact, is attained in nearly all cases somewhere between the photosphere and the region of appreciable hydrogen ionization. (It is interesting to note the very large values attained by $\nabla_r (\sim 20$ to 50) in some cases; these values would actually obtain if convection were too inefficient to exert any "smoothing" influence on the temperature gradient. Since ∇_r may also be interpreted as the ratio of the pressure to the temperature scale heights (if pure radiative transfer obtains), it follows that in these regions of very large ∇_r the temperature scale height is only a few per cent of the pressure scale height; hence the temperature may change by a factor of two, *e.g.*, in only a small fraction of a pressure scale height.) At temperatures somewhat above $10^4\,°\mathrm{K}$, where hydrogen is mostly ionized, the opacity must begin to decrease with increasing temperature because the electron density in these regions is now relatively insensitive to temperature (*i.e.*, s must increase and become positive). In these deeper regions bound-free contributions from helium and heavier elements become important and the opacity begins to acquire a "Kramers-like" behavior (*i.e.*, n and s positive or zero, say). Hence ∇_r should generally begin to decrease in value at temperatures somewhat above $10^4\,°\mathrm{K}$.

Table 20.4

VALUES OF $f(T, T_e)$ (*cf.* (20.35))

$T_e(10^3\,°\mathrm{K})$	$T(10^3\,°\mathrm{K})$					
	$T=T_e$	3.60	5.04	7.50	9.00	10.08
2.29	1	2.385	3.386	3.890	3.935	3.948
2.80	1	1.796	2.781	3.261	3.304	3.312
3.60	1	1	2.048	2.514	2.555	2.567
5.04	1		1	1.322	1.350	1.358
7.00	1			1.116	1.272	1.314
8.00	1				1.174	1.261
10.00	1					1.0162

If effective convection has set in by the time T has reached $\sim 10^4\,°\mathrm{K}$, the behavior of ∇_r (now the "fictitious radiative gradient") will be altered (*cf.* Chap. 14). Note also that for given T, ∇_r decreases with increasing T_e. This is primarily a result of the increasing proximity of the photosphere to the region of interest as T_e increases. For example, for $T = 10{,}080\,°\mathrm{K}$ (in or near the region of appreciable hydrogen ionization), values of ∇_r are quite small for $T_e \gtrsim 10{,}000\,°\mathrm{K}$; any convective instability present in the envelopes of these hotter stars will probably be caused more by some abundant element (hydrogen and/or helium) undergoing ionization and thereby lowering the value of ∇_{ad} than by some property of the opacity increasing the value of ∇_r.

Secondly, we note that over the range of temperatures of interest to us at present, the function $f(T,T_e)$ (*cf.* (20.35)) is a slowly varying function of both T and T_e, particularly for $T \geq 5040\,°\mathrm{K}$ (for which $n+s+4<0$). This suggests that the pressure at some point between the photosphere and the hydrogen-ionization region (for example, at the point at which convection may become effective) is not very sensitive to the exact temperature at that point and, furthermore, that this pressure is roughly proportional to P_p, the photospheric pressure, which depends (for a given opacity law) only on g_s and T_e (this approximate proportionality to P_p should really be restricted to the case $n+s+4 \leq 0$, *cf.* next paragraph).

Assuming that T is appreciably larger than T_e, we have from (20.35)–(20.37) the following approximate expressions for the pressure at some temperature T:

$$P \simeq \left\{ \frac{n+1}{n+s+4} \cdot \frac{16}{3} \frac{g_s}{\kappa_0' T_e^4} T^{n+s+4} \right\}^{\frac{1}{n+1}} \qquad (n+s+4>0), \quad (20.60)$$

$$P = \left\{ (n+1) \cdot \frac{16}{3} \frac{g_s}{\kappa_0' T_e^4} \cdot \ln\left(\frac{2^{1/4} T}{T_e} \right) \right\}^{\frac{1}{n+1}} \qquad (n+s+4=0), \quad (20.61)$$

$$P \simeq \left\{ \frac{n+1}{|n+s+4|} \cdot \frac{16}{3} \frac{g_s}{\kappa_0'} \cdot \frac{2^{\frac{|n+s+4|}{4}}}{T_e^{|n+s|}} \right\}^{\frac{1}{n+1}} \qquad (n+s+4<0). \quad (20.62)$$

Thus we see (neglecting the slowly varying logarithmic term in (20.61)) that the pressure at some given temperature T appreciably larger than T_e is given by

$$P \propto (g_s/T_e^4)^{1/(n+1)} \quad (20.63)$$

for $n+s+4 \geq 0$ (where the factor of proportionality depends on T) and by

$$P \propto (g_s/T_e^{|n+s|})^{1/(n+1)} \quad (20.64)$$

for $n+s+4<0$, *i.e.*, for $|n+s|>4$ (where the factor of proportionality is

practically independent of T). The important conclusion to be drawn from these considerations is that the pressure (and hence also the density) at a given temperature (considerably larger than T_e) in the envelope generally decreases strongly with increasing effective temperature and increases rather weakly with increasing surface gravity. The first of these effects arises, physically, from either of two factors. For cooler stars, for which κ increases strongly with increasing temperature T, the resulting steep temperature gradient implies that the pressure is not very sensitive to the temperature on the steep portion of the curve. The pressure at a given temperature is therefore essentially proportional to the photospheric pressure, which in turn decreases with increasing effective temperature T_e because of the rapid increase of κ_p with increasing T_e (recall that, approximately, $P_p \propto g_s/\kappa_p$ and $\kappa_\rho \propto P_p^{\,n} T_e^{\,-n-s}$). For hotter stars (say with T_e near 10,000 °K), for which κ does not increase so strongly (or perhaps even decreases) with increasing T (say for which $n+s+4>0$), the pressure depends more sensitively on T and the photospheric pressure may actually increase with increasing T_e. The pressure at a given T now depends more sensitively on how "far" the photosphere is away from the point in question, however, and clearly decreases as the photosphere approaches the level in question. The second of these effects (dependence on surface gravity) arises essentially from the fact that the pressure at a given T, being proportional to the weight of the overlying layers, increases with increasing surface gravity g_s. Note that the specific entropy at a given T generally increases strongly with increasing T_e and decreases less strongly with increasing g_s.

These considerations will prove useful in the next section.

20.5 Regions on the H-R Diagram Where Convection in Stellar Envelopes is Effective

We have seen that stars of "normal" composition (*i.e.*, composed predominantly of hydrogen) with $T_e \lesssim 10^4$ °K are unstable against convection in the regions *above* the hydrogen ionization region because of the rapid inward increase of the opacity, and *in* the hydrogen ionization region both because of this and because of the small values of the adiabatic gradient ∇_{ad} resulting from the ionization of hydrogen (*cf.* Sect. (9.18) and (18.8′)). Stars with T_e somewhat greater than 10^4 °K are probably also unstable against convection at or immediately beneath their photospheres, but now primarily because of the small values of ∇_{ad} rather than of any excessively large values of ∇_r. In both cases the He^+ ionization region may be unstable against convection if sufficient helium is present (say more than 10 per cent of the hydrogen abundance, by numbers), because of the effect of the ionization of

He^+ in diminishing the values of ∇_{rad}. In stars with T_e considerably greater than 10^4 °K, in which hydrogen is essentially fully ionized everywhere in the star, convective instability can only exist in the ionization zones of He and He^+, since there is now no reason to expect the opacity to increase strongly inward outside of these zones (it can be seen from Fig. 16.5 that, while n in the opacity law (20.24) is always close to unity in the helium ionization zones, s may for certain densities be slightly negative in the second helium ionization zone). Only in stars with $T_e > \sim 5 \times 10^4$ °K (where hydrogen and helium are both essentially fully ionized throughout) can one expect the entire envelope to be stable against convection; such stars could in principle be purely radiative in their outer layers all the way to the surface.*

We conclude that, for one reason or another, essentially all stars of "normal" composition with $T_e < \sim 4 \times 10^4$ °K (later than, say, O3) are convectively unstable somewhere in their outer layers. Why, then, do not all such stars have convective envelopes? The crucial point is the *effectiveness* of convection in the envelope. We shoul ask, in which stars can the convective instability lead to a (possibly deep) convection zone in which an appreciable fraction of the total energy is carried by convection?

Possibly the best approach to the answer is the following: Assume values of chemical composition, L, M, and R appropriate for stars in different regions of the H-R diagram; then integrate the equations of radiative transfer through the atmosphere (usually assumed grey), using realistic opacities, until a point of instability against convection is reached. Then, using a theory of convection such as the Böhm-Vitense mixing-length theory (*cf.* Chap. 14), carry the solution down through the convectively unstable regions (which will be considerably extended if convection has become effective, *cf.* Sect. 20.6b) to the point (if it exists) where the material is again stable against convection. These calculations should indicate which stars have effective convective envelopes. The main uncertainty here is, aside from the intrinsic uncertainty in the mixing length theory itself, in the value to be used for the mixing length Λ. In the cooler stars (say $T_e \lesssim 7000$ °K), the computed depth of the convection zone is quite sensitive to the value of Λ.

Such calculations have been carried out by Böhm-Vitense [Bö58] for fairly widely distributed points on the H-R diagram, and by Baker [Ba63, 64b] for points confined along and near the Population I main sequence. In both cases the calculations showed that stars cooler than some "transition" effective temperature (which depends on surface gravity g_s as well as on other quantities) have deep and effective convection zones in their envelopes, and

* Actual O and B stars, however, evidently are not generally in simple radiative, hydrostatic equilibrium in their outer layers; see, for example, Underhill [Un60].

the depth of these zones increases with decreasing effective temperature T_e; stars hotter than this transition temperature have only thin and ineffective convection zones. The following tabulation shows the results of Böhm-Vitense (private communication, 1964):

Luminosity Class	*Convection Ineffective for* $T_e >$	*Spectral Class*
V	7500 °K	A7
III	6500 °K	F5
II	5000 °K	G2
Ia	4000 °K	K0

Some of Baker's [Ba63,64b] results are reproduced in Fig. 20.1, in which the fractional thickness $\Delta r/R$ (R = stellar radius) of the convection zone is plotted against effective temperature T_e along the zero-age main sequence, for several values of α, the mixing length-pressure scale height ratio. The composition adopted by Baker was a "Population I" composition, $X = 0.70$, $Y = 0.27$, $Z = 0.03$; and the values of luminosity L and radius R adopted by Baker for each mass M are given to better than 10 per cent for L and to better than 5 per cent for R by the formulae

$$\log L = 4.47 \log M - 0.03,$$

$$\log R = 0.89 \log M - 0.006,$$

where L, M, and R are in solar units. It is seen from Fig. 20.1 that for $\alpha = 1.5$, Baker's value of the "transition" effective temperature, above which the convection zone is very thin and ineffective in zero-age main sequence stars, is about 7300 °K, in adequate agreement with Böhm-Vitense's results.

In order to obtain a somewhat intuitive understanding of these results, we shall adopt a simplified picture of convective transfer. This picture has been used by a number of authors (Hoyle and Schwarzschild [Ho55], Hayashi *et al.* [Ha62a], for example) and it can be related to the mixing-length theory of convection (*cf.* Chap. 14). To obtain this picture, we start with the expression which was derived in Chap. 14 on the basis of the mixing-length theory for the average convective flux:

$$F_c = (1/2)\rho \bar{v} c_P \Delta T \tag{20.65a}$$

$$= \left[\frac{1}{2}\left(\frac{\bar{v}}{v_S}\right)\left(\frac{\Delta T}{T}\right)\right] \rho v_S c_P T \tag{20.65b}$$

$$\equiv \eta \cdot \rho v_S c_P T. \tag{20.65c}$$

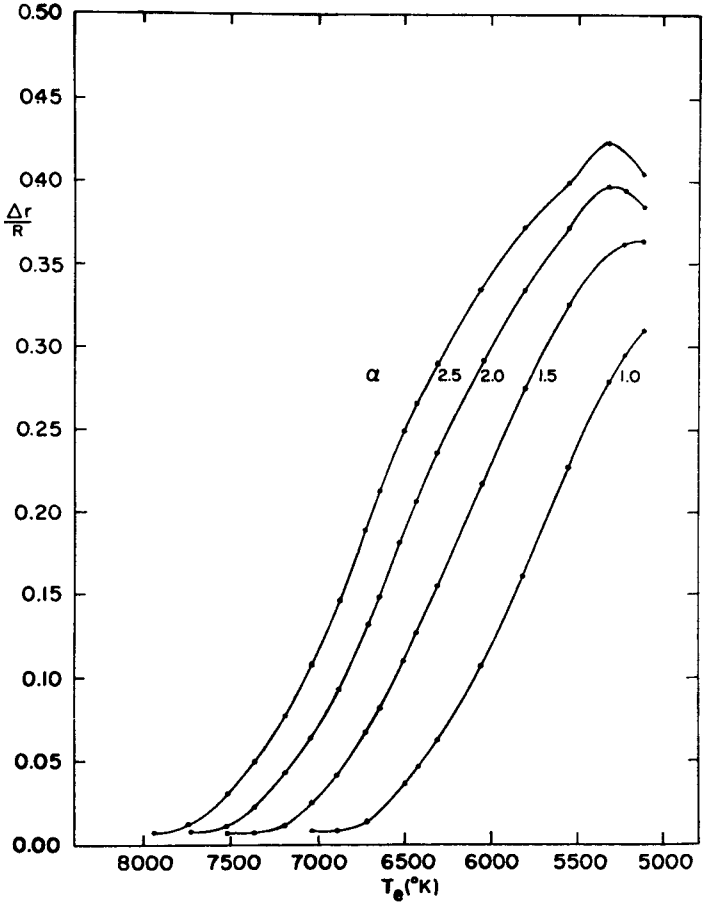

Fig. 20.1 Fractional thickness $\Delta r/R$ of convective envelopes vs. effective temperature T_e for zero-age main sequence stars (from Baker [Ba63,64b]). Each curve corresponds to a labelled value of α, the ratio of the mixing length to the pressure scale height.

Here ρ is the density, $\bar{v}$ is the average convective velocity over one mixing length, c_P is the specific heat per unit mass at constant pressure, ΔT is the average excess of a convecting element over the average of its surroundings after having moved through one mixing length, and v_S denotes the local Laplacian (adiabatic) velocity of sound:*

$$v_S = \sqrt{\Gamma_1 P/\rho} = \sqrt{\Gamma_1(\mathscr{R}/\mu\beta)T}, \tag{20.66}$$

* See the fourth footnote in Sect. 14.3 for the appropriate relativistic generalization of (20.66).

where Γ_1 is defined in Sect. 9.14. In the second equality in (20.66) we have assumed a "modified" perfect gas equation of state of the form

$$P=\frac{\mathscr{R}}{\mu\beta}\rho T, \tag{20.67}$$

where $\beta = P_g/(P_g+P_r)$ is the ratio of gas to total (gas plus radiation) pressure, $\mathscr{R}$ is the gas constant per mole, and μ is the mean molecular weight of the material. In (20.65c) the value of the factor η could, in principle at least, be computed from the mixing-length theory, and its value would be found to depend strongly on local physical conditions. For example, using the order-of-magnitude values derived in Sect. 14.6, we find that $\eta\sim(t_{\rm ff}/t_K)\sim 10^{-12}$ or so in the deep interior and $\eta\sim 10^{-1}$ in the outermost stellar layers. The simplified picture consists in ignoring this dependence of η on local physical conditions and regarding η as a sort of constant "efficiency factor" whose value is simply assumed. (We note that $\eta<(1/2)$ even if $\bar{v} = v_S$, since $\Delta T/T$ is always less than unity under realistic conditions.) Taking η and c_P as constant, then, we see that the convective flux $F_c\propto\rho T^{3/2}\propto PT^{1/2}$ for an equation of state of the form (20.67) and thus depends only weakly on T if P (rather than ρ) is regarded as the other independent thermodynamic variable.

The *total* flux, on the other hand, is

$$F_{\rm total}=(R/r)^2\cdot\sigma T_e^4, \tag{20.68}$$

where r denotes radial distance, R the stellar radius, σ the Stefan-Boltzmann constant, and T_e the effective temperature. We now define f as the ratio of the convective to the total flux:

$$f\equiv\frac{F_c}{F_{\rm total}}=\left(\frac{r}{R}\right)^2\frac{\eta c_P\rho T v_S}{\sigma T_e^4}. \tag{20.69}$$

We are going to regard f as a measure of convective efficiency, such that $f\ll 1$ corresponds to inefficient convection, $f\sim 1$ to efficient convection. The relation between f and the dimensionless parameter A (ratio of the "convective" to the "radiative" conductivities, introduced in Chap. 14, see (14.70), (14.98), and (14.99)), and hence the justification for regarding f as an efficiency parameter, will be obtained at the end of this section.

We use the equation of state (20.67) to express ρT in terms of P, (20.66) for v_S, and write

$$c_P=\left(\frac{5}{2}\frac{\mathscr{R}}{\mu}\right)\left(\frac{2c_P\mu}{5\mathscr{R}}\right) \tag{20.70}$$

(since $5\mathscr{R}/2\mu$ is the value of c_P for a perfect monatomic gas with $\beta = 1$); (20.69) then becomes

$$f=\frac{5}{2}\eta\left(\frac{r}{R}\right)^2\left(\frac{\Gamma_1\mathscr{R}}{\mu\beta}\right)^{1/2}\left(\frac{2c_P\mu\beta}{5\mathscr{R}}\right)\frac{PT^{1/2}}{\sigma T_e^4}. \tag{20.71}$$

We must now consider the dependence of P on g_s, T_e, and T. We shall examine the convective efficiency of a region in or immediately above the hydrogen ionization region, since the material is likely to be highly convectively unstable here (*i.e.*, $\nabla_r \gg \nabla_{ad}$). Calculations (for example, Baker [Ba63,64b]) show that, if convection is not effective in the hydrogen ionization region, it is usually not effective in the He^+ ionization region either. Presumably this is because, in spite of the higher densities in the He^+ ionization zone, the material is not strongly unstable against convection in this zone (*i.e.*, $\nabla_r - \nabla_{ad}$ is not very large), provided that the material above this zone is in radiative equilibrium. We shall also use the $P(T)$ relation which applies in the case of pure radiative transfer, in evaluating f at the level in question. The equation ((20.73) below) that we obtain for f will then not be strictly valid if f as given by this equation should turn out to be larger than unity. In regions of strong convective instability, however, the purely radiative $P(T)$ relation always yields (for given photospheric conditions) smaller values of P, for given T, than the correct $P(T)$ relation which applies to cases where both radiation and convection contribute to the flux. Our equation for f therefore *underestimates* the values of f that would be given if the "correct" (but unknown) $P(T)$ relation were to be used in place of the purely radiative relation. The factor by which (20.73) underestimates the "true" value of f is probably always less than 10; this is adequate accuracy for our present purposes.

Since we know from Baker [Ba63,64b] that the transition effective temperature for main sequence stars is $\sim 7500°K$, we use (20.54) and the purely radiative $P(T)$ relation (20.37), valid for $T \gtrsim 5000°K$, in which $n+s+4<0$. Assuming T to be considerably larger than T_e, we thus have

$$P(T)\simeq\left\{\frac{n+1}{|n+s+4|}\cdot\frac{16}{3}\frac{g_s}{\kappa_1'}\frac{2^{|n+s+4|/4}}{T_e^{|n+s|}}\right\}^{\frac{1}{n+1}}, \tag{20.72}$$

whence (20.71) becomes

$$f=\frac{5}{2}\eta\left(\frac{r}{R}\right)^2\left(\frac{\Gamma_1\mathscr{R}}{\mu\beta}\right)^{1/2}\left(\frac{2c_P\mu\beta}{5\mathscr{R}}\right)$$

$$\cdot T^{1/2}\left\{\frac{n+1}{|n+s+4|}\cdot\frac{16}{3}\frac{2^{|n+s+4|/4}}{\kappa_1'}\right\}^{\frac{1}{n+1}}\cdot\frac{g_s^{\frac{1}{n+1}}}{\sigma T_e^{4+\frac{|n+s|}{n+1}}}, \tag{20.73}$$

where (see(20.55) and (20.56)) for a "Population I" composition ($X = 0.61$, $Y = 0.37$, $Z = 0.02$)

$$\kappa_1' = 10^{-15.58}(5040)^{3.05+0.74+s}. \tag{20.74}$$

For simplicity, we shall adopt $n = 1$, $s = -10$ (although $n = 0.74$ is implied by (20.74)); then $n+s = -9$, $n+s+4 = -5$, and $\kappa_1' = 10^{-37.6}$. With these values, (20.73) becomes

$$f \simeq 7.4 \times 10^{29} \eta \left(\frac{r}{R}\right)^2 \left(\frac{3\Gamma_1}{5\mu\beta}\right)^{1/2} \left(\frac{2c_P\mu\beta}{5\mathscr{R}}\right) \left(\frac{T}{10^4}\right)^{1/2} \frac{g_s^{1/2}}{T_e^{17/2}}, \tag{20.75}$$

where c.g.s. units are used throughout. We note that f increases slowly with increasing g_s and decreases *very* rapidly with increasing T_e. This behavior of f occurs because $F_c \propto P \propto g_s^{1/2}/T_e^{9/2}$ (for given T) and $F_{\text{total}} \propto T_e^4$. We see that, because of the large value of the exponent of T_e, the transition from $f \ll 1$ (ineffective convection) to $f \sim 1$ (effective convection) is extremely rapid and occurs within a fairly well-defined, narrow range in T_e and is not very sensitive to g_s. For main sequence stars not greatly different from the sun we may take $g_s \simeq 3 \times 10^4$ cm/sec^2 (approximately the solar value), since it may easily be shown that g_s varies only very slowly along the main sequence (decreasing slowly toward earlier spectral types). We also take $T \simeq 10^4$ °K since (as was pointed out earlier) this is probably close to regions of large convective instability. Because hydrogen is probably partially ionized here, we shall take $(2c_P\mu\beta/5\mathscr{R}) \simeq 20$, since (see the latter part of Sect. 9.18) hydrogen ionization (if hydrogen is a dominant element) can increase the value of c_P by a factor of 20–30. We also take $\Gamma_1 \simeq (5/3)$, $\mu \simeq 1$, $\beta \simeq 1$, $(r/R) \simeq 1$, and $\eta \simeq 0.1$. Defining the "transition" effective temperature to correspond to $f = 0.5$ (half of total flux carried by convection in the hydrogen ionization region), we can solve (20.75) for this value of T_e. We obtain $T_e \simeq 7.0 \times 10^3$ °K, in surprisingly good agreement with values obtained by Baker [Ba63,64b], and by Böhm-Vitense. We note that, because of the large value of the exponent of T_e in (20.75), the result is not very sensitive to the exact values used for the various parameters.

We may also extend this result to non-main sequence stars by considering lines of constant convective efficiency, *i.e.*, lines along which $f = const.$ From (20.75) we obtain for the relation between T_e and g_s along a line of constant f

$$T_e \simeq 7.0 \times 10^3 \left(\frac{\eta}{0.1}\right)^{2/17} \left(\frac{r}{R}\right)^{4/17} \left(\frac{0.5}{f}\right)^{2/17} \left(\frac{3\Gamma_1}{5\mu\beta}\right)^{1/17} \cdot \left(\frac{1}{20} \cdot \frac{2c_P\mu\beta}{5\mathscr{R}}\right)^{2/17} \left(\frac{T}{10^4}\right)^{1/17} \left(\frac{g_s}{3 \times 10^4}\right)^{1/17} \text{°K}. \tag{20.76}$$

Hence, for constant values of $\eta, f, T, r/R$, etc., we have

$$T_e = \text{const.}\, g_s^{\alpha}, \tag{20.77}$$

where $\alpha \simeq (1/17)$ in this crude approximation. It can be deduced from the tabulation at the beginning of this section that a value $\alpha \simeq (1/13)$ in (20.77) will reproduce Böhm-Vitense's results. Considering the crudity of our approximations, this may be considered satisfactory agreement.

We note that the lines of constant convective efficiency are almost vertical ($T_e \simeq const.$, almost independent of g_s) on an H-R diagram, but that they do slant slightly to the right, since g_s decreases as luminosity L increases (see Fig. 20.2). Assuming that $L \propto M^4$, it is easy to show that, if $T_e \propto g_s^{\alpha}$, then

$$L = \text{const.}\, T_e^{-\gamma}, \tag{20.78a}$$

where

$$\gamma = \frac{4}{3}\left(\frac{1}{\alpha} - 4\right).$$

We have $\gamma = 17.3$ if $\alpha = (1/17)$ (our value) and $\gamma = 12$ if $\alpha = (1/13)$ (Böhm-Vitense's value). Equation (20.78a) is the equation of a locus $f = const.$ on the H-R diagram.

Noting from Fig. 20.2 that the line $f = 0.5$ crosses the main sequence at about spectral type A7V, we may evaluate the constant in (20.78a) from the information given in Chap. 0. Equation (20.78a) may then be written in the form

$$\left(\frac{L}{10}\right) = \left(\frac{T_e}{7600}\right)^{-\gamma} \qquad (f = 0.5), \tag{20.78a'}$$

where L is in solar units and T_e is in °K.

We may conclude from these results that all stars lying to the right of the locus in the H-R diagram corresponding to, say, $f = 0.5$ (see Fig. 20.2) have effective convection zones in their envelopes. Stars lying to the left of this locus essentially have purely radiative envelopes (*i.e.*, any convection zones present will be thin and ineffective and can be disregarded as far as the structure of the star is concerned).

To summarize the argument briefly: We showed that in the region where the temperature gradient is extremely steep (owing to the rapid inward increase of the opacity), the pressure P is not very sensitive to the value of the temperature T in this region (simply *because* of the steep gradient). Therefore

$$P \propto P_g,$$

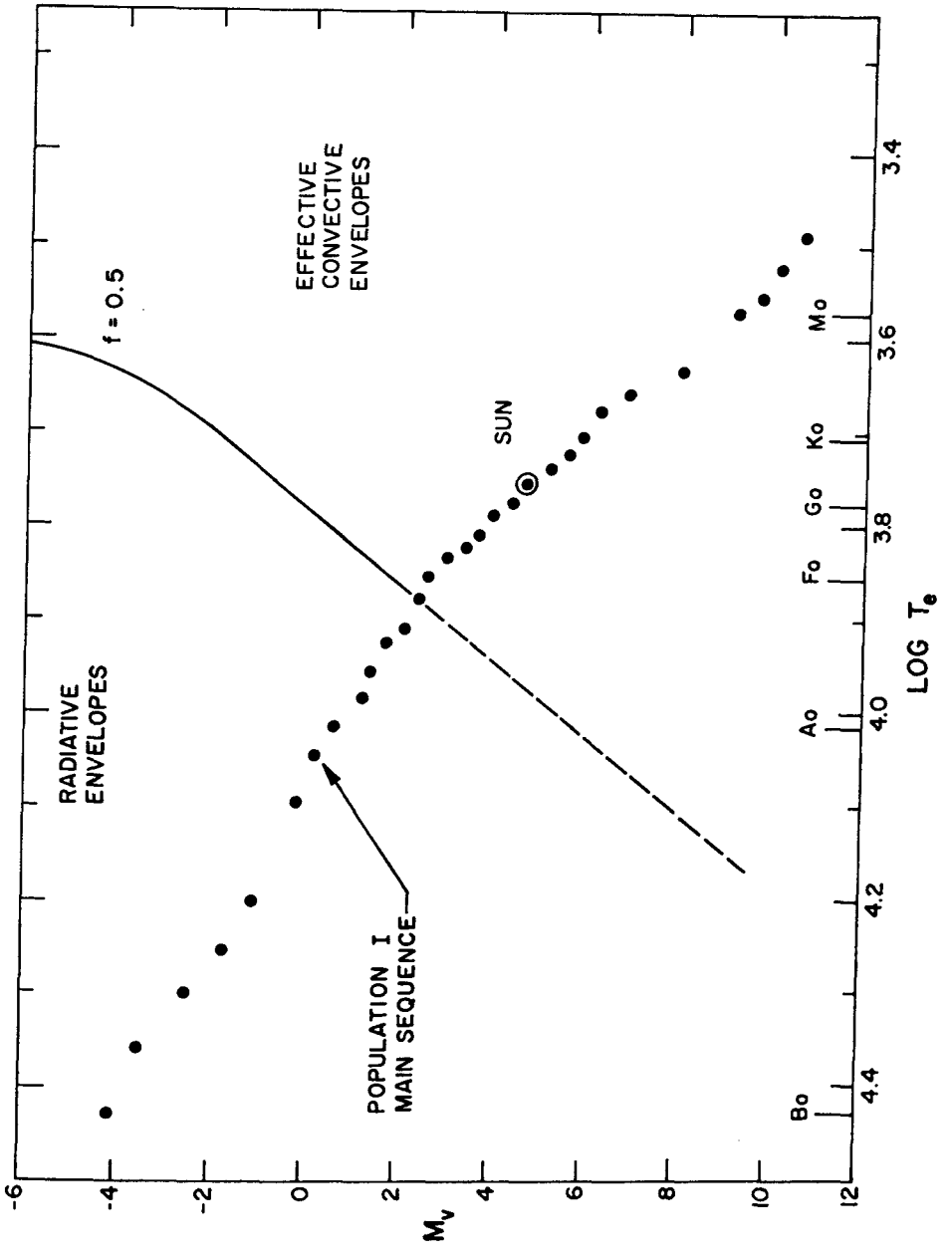

Fig. 20.2 Regions on the H-R diagram where convection is expected to be effective in stellar envelopes. The results of Böhm-Vitense (see tabulation at beginning of this section) have been used for the $f = 0.5$ locus. The main sequence points were obtained from Keenan [Ke63].

where P_p is the photospheric pressure (at $\tau = (2/3)$):

$$P_p \sim \frac{g_s}{\kappa_p},$$

κ_p being the photospheric value of the opacity. Assuming that $\kappa \propto PT^9$, say, in the relevant regions, we have

$$P_p \propto \frac{g_s}{P_p T_e^9},$$

which gives

$$P_p \propto \frac{{g_s}^{1/2}}{T_e^{9/2}}.$$

Since, approximately, $F_c \propto PT^{1/2} \propto P_p T^{1/2}$, where F_c is the convective flux, we have

$$F_c \propto T^{1/2} {g_s}^{1/2} / T_e^{9/2}.$$

On the other hand, the total flux is $F_{\text{tot}} \propto T_e^4$ (for $r/R \simeq 1$), whence

$$f = F_c/F_{\text{tot}} \propto T^{1/2} {g_s}^{1/2} / T_e^{17/2},$$

which, aside from the factor of proportionality, is (20.75).

All the above discussion has been for stars of Population I. However, because of the smallness of the exponent α, the corresponding results for Population II stars will not be significantly different from the above.

As is shown by the calculations of Baker [Ba63,64b] (see Fig. 20.1) and Böhm-Vitense [Bö58], and as we shall see in Sect. 20.6, the depth of the outer convection zone increases from a small fraction of the radius for main sequence stars in or near the transition region to ~ 15 per cent for the sun until, according to Limber [Li58], the stars become completely convective in the late M spectral class (*cf.* Sect. 26.3). However, the calculations of Baker [Ba63,64b] imply that the temperatures at the bottoms of the convection zones may reach an upper limit and therefore that there may be some possibility that the late M stars are not convective all the way to the center.

Some semi-empirical evidence that the late type stars develop deep convective envelopes at least during their gravitational contraction to the main sequence will be presented in Sect. 26.1b.

We consider, next, the relation between f, the ratio of the convective to the total flux, and the dimensionless parameter A (ratio of "convective" to "radiative" conductivities, see Chap. 14). There it was shown that A could be regarded, roughly, as an efficiency parameter for convective transfer, such that $A \gg 1$ implies efficient convection, while $A \ll 1$ implies inefficient con-

vection. We shall now justify our use of f as a convective efficiency parameter. From (14.98) we have the following expression for A:

$$A=\frac{4}{9}\frac{(Q^{1/2}/4\sqrt{2}\,\Gamma_1^{1/2})\rho v_S c_P T\alpha^2}{(4ac/3)(T^4 g/\kappa P)}, \tag{20.78b}$$

where α is the mixing length-pressure scale height ratio and the other symbols are as defined in Chap. 14. We note in (20.78b) that $\rho v_S c_P T = F_c/\eta$ (*cf.* (20.65c)). We also have the following expression for the fictitious radiative gradient (*cf.* (20.21′)):

$$\nabla_r \equiv \left(\frac{\mathrm{d}\ln T}{\mathrm{d}\ln P}\right)_{\mathrm{rad}} = \frac{3}{16}\frac{\kappa P}{T^4}\left(\frac{L_r}{L}\right)\left(\frac{R}{r}\right)^2\frac{T_e^4}{g}. \tag{20.78c}$$

Using the expression $F_{\mathrm{total}} = (R/r)^2\sigma T_e^4$, we can solve (20.78c) for the quantity

$$\frac{4ac}{3}\frac{T^4 g}{\kappa P} = \left(\frac{L_r}{L}\right)\frac{F_{\mathrm{total}}}{\nabla_r} \tag{20.78d}$$

which enters into the denominator of (20.78b) for A. Equation (20.78b) then becomes

$$A=\frac{Q^{1/2}\alpha^2}{9\sqrt{2}\,\Gamma_1^{1/2}}\left(\frac{L}{L_r}\right)\nabla_r\frac{f}{\eta}, \tag{20.78e}$$

which is the desired relation.

Under most stellar envelope conditions the factor multiplying $\nabla_r f/\eta$ is of order unity. Assuming, moreover, ∇_r to be of order unity, we have the order-of-magnitude relation

$$A\sim f/\eta.^{*} \tag{20.78f}$$

It then follows that, aside from effects arising from a possible variation of ∇_r, A is of the same order of magnitude as f/η and has essentially the same dependence on stellar parameters (such as T_e, g_s, T) as does f/η (see (20.75)). Hence, if $f/\eta \gg 1$, then $A \gg 1$ and convection, if it occurs, can be efficient. Similarly, if $f/\eta \ll 1$, then $A \ll 1$ (unless ∇_r happens to be extremely large) and any convection present will be inefficient. Moreover, if the variation of ∇_r with stellar parameters is ignored, it is seen that with η assumed constant, lines of constant f are also essentially lines of constant A, Q.E.D.

We note that, writing

$$F_c^{\max} \equiv \rho v_S c_P T \tag{20.78g}$$

* Assuming that $f\sim 1$ and using the order-of-magnitude expression $\eta\sim(t_{\mathrm{ff}}/t_k)$ (see the discussion following (20.67)), valid in the deep interior, we have $A\sim(t_{\mathrm{ff}}/t_k)^{-1}$ in the deep interior, as was also obtained in Sect. 14.7.

as the "maximum possible convective flux" (a considerable overestimate in practically all cases!), we can also write

$$\eta = F_c/F_c^{\max}. \tag{20.78h}$$

We note that $F_c^{\max}$ is the convective flux which would correspond to mean convective velocities equal to the sonic velocity; such convective velocities, in turn, imply that $(\Delta T/T)\sim 1$ (since, in general, $(\bar{v}/v_S)\sim(\Delta T/T)^{1/2}$ if $\alpha \sim 1$, *cf.* Chap. 14). Using (20.78h) in (20.78f), we see that

$$A \sim F_c^{\max}/F_{\text{total}}, \tag{20.78i}$$

which provides another interpretation of A. If $A \gg 1$ (as is normally true in the deep interior, see the preceding footnote), then the maximum possible convective flux is much larger than the total actual flux (convective plus radiative); hence the flux could easily be practically wholly convective if conditions demanded that it be so. If, on the other hand, $A \ll 1$, then non-supersonic convection could never account for more than a small fraction of the total flux.

Finally, we recall that a large value of f/η, and hence (assuming that $\nabla_r \sim 1$) a large value of A, do not necessarily always imply that $f \simeq 1$. However, unless $\nabla_r - \nabla_{ad} \ll 1$, $A \gg 1$ implies that B (*cf.* (14.81)) $\gg 1$, which in turn implies that $\zeta \equiv (\nabla_r - \nabla)/(\nabla_r - \nabla_{ad})$ (*cf.* Sect. 14.7) $\simeq 1$ (efficient convection in the sense of Chap. 14). We have (*cf.* (14.43))

$$f = \frac{\nabla_r - \nabla_{ad}}{\nabla_r}\zeta, \tag{20.78j}$$

so that $f \leq \zeta$ always and $f \simeq (\nabla_r - \nabla_{ad})/\nabla_r$ if $\zeta \simeq 1$. This last relation shows that f can approach unity when $A \gg 1$ if ∇_r is several times ∇_{ad}. If $A \ll 1$, then $B \ll 1$ (unless $\nabla_r - \nabla_{ad} \gg 1$) and hence $\zeta \ll 1$ (inefficient convection in the sense of Chap. 14). From (20.78j), then, it follows that $f \ll 1$ and only a small fraction of the total flux is convective.

20.6 Stellar Envelopes in Convective Equilibrium

As we have seen in Sect. 20.5, all stars of "normal" chemical composition (*i.e.*, predominantly hydrogen) whose effective temperatures T_e are lower than some "transition" temperature (which is about 7500°K for main sequence stars, *i.e.*, about spectral type A7) are expected to have effective convection zones beginning immediately beneath their photospheres and extending (perhaps) deep into the interior. There exists some semi-empirical evidence, to be discussed in Sect. 26.1b, which suggests that deep and

effective convective envelopes indeed develop in late type stars. We consider in this section the general structure of such convective envelopes and some of their properties.

20.6a Preliminary Considerations

It is clear that if a good theory of convective transfer existed, one could compute the complete structure of such an envelope simply by using this theory to integrate the stellar structure equations from the point where the material first becomes convectively unstable ($\nabla_r \geq \nabla_{ad}$) down through the convection zone to the point (if it exists) where the material is again stable against convection ($\nabla_r < \nabla_{ad}$). The best theory of convection available at present seems to be the Böhm-Vitense mixing-length theory [Vi53, Bö58], which we have described in Chap. 14. We have also noted that calculations employing this theory have been carried out, for example, by Böhm-Vitense [Bö58] and by Baker [Ba63,64b], and we have summarized some of their results in Sect. 20.5. These calculations are quite complex, however, and it is useful to consider simpler, more approximate methods of calculation which have been used in the past and which provide insight into the physical factors which determine the structure of convective envelopes.

The first simplification is based on the fact, which we noted in Chaps. 13 and 14, that the excess of the superadiabatic gradient (which is really just the actual gradient, ∇) over the adiabatic gradient ∇_{ad} becomes smaller and smaller as one descends into a convection zone. (In the language of Chap. 14, the parameter A generally increases with increasing depth in a stellar envelope, *cf.* Sect. 14.7.) Let us refer to the outermost region of a convection zone, where the excess of the superadiabatic gradient over the adiabatic is appreciable, as the "transition region." Its detailed structure depends critically on the theory of convection which is being used; for example, in the case of the mixing-length theory, the value used for the mixing length Λ plays a decisive role in determining the detailed structure of this region. In the regions below the transition region (assuming that they exist and are unstable against convection), the superadiabaticity of the gradient will be small and for this reason, as we have seen (Chaps. 13 and 14), the structure of the region becomes insensitive to the theory of convection which is being used. In such regions the structure can often be approximated by neglecting this superadiabaticity and simply setting the actual gradient equal to the adiabatic:

$$\nabla = \frac{d \ln T}{d \ln P} = \nabla_{ad} = \frac{\Gamma_2 - 1}{\Gamma_2}, \tag{20.79}$$

where Γ_2 can be computed at each point from knowledge of the local values of ρ, T, and chemical composition (see Chap. 9 and (18.8′)). Equation

(20.79) can then be integrated through the region to yield P as a function of T.

It should be noted that in the approximation (20.79) and in the absence of irreversible processes (see (13.31) and the discussion following this equation), the specific entropy S is *constant* with depth in the convection zone. Because, however, ∇ is always slightly larger than ∇_{ad} in an actual convection zone containing no nuclear energy sources, S actually always increases inward somewhat in such convection zones.

In dwarfs later than, say, G0 the transition region is likely to be thin (*cf.* Baker [Ba63,64b]) and one sometimes neglects it entirely, using (20.79) throughout the entire convectively unstable region. In giant and supergiant stars, however, the transition region is likely to occupy a considerably larger fraction of the convection zone than in the dwarfs, so that use of (20.79) throughout the convection zone may introduce a large error.

If Γ_2 is constant in the regions of interest, then (20.79) can be integrated at once to give

$$P \propto T^{\Gamma_2/(\Gamma_2-1)}, \tag{20.80}$$

which may be written in the form

$$P = KT^{n_e+1}, \tag{20.81}$$

where

$$n_e = 1/(\Gamma_2 - 1), \tag{20.82}$$

and where K is a constant of integration whose value is determined by the values of P and T at the bottom of the transition region. If the transition region is neglected, then the value of K would be determined by the values of P and T at the point where convective instability first sets in; sometimes photospheric values of P and T are used, since the point where convective instability first occurs is usually rather close to the photosphere (*cf.* Sect. 20.4). In this last case, then, the computation of a stellar atmosphere is required (although a simple grey atmosphere is usually assumed) in order to evaluate K. Sometimes even the atmosphere is neglected and the simple "zero" boundary conditions $T = 0$ and $P = 0$ at $r = R$ (the stellar radius) are used. In the last case it is clear that the value of K is not determined at all by the boundary conditions (assuming that the star is not completely convective, *cf.* Sect. 22.5) and K must be regarded as an additional constant of integration. In this case K is sometimes simply regarded as a free parameter whose value is chosen so as to give a reasonable fit to observations. For example, models of stars with convective envelopes have been computed (*cf.*, for example, Schwarzschild [Sc58b, Chap. 4]) by ignoring the hydrogen

and helium ionization zones, setting $\Gamma_2 = (5/3)$, and using the zero boundary conditions $P = 0$ and $T = 0$ at $r = R$. Equation (20.81) then becomes

$$P = KT^{2.5}, \tag{20.83}$$

where K is now regarded as a free parameter. In this case we see from our considerations of the Vogt-Russell (V-R) theorem (*cf.* Sect. 18.1) that now the value of K must be specified, in addition to the values of mass M and chemical composition, in order for the structure of the star to be determined. If L, M, and R are assumed known, then the value of K is adjusted until a reasonable chemical composition for the model is derived; in this way the value of K may be considered as determined by observation. As we shall see later in this section, the value of K determines the depth of the convective envelope.

Even if Γ_2 is not constant (as in the hydrogen and helium ionization zones, for example), (20.79) can still often be integrated analytically by making use of the constancy of the entropy along an adiabat (*cf.* Limber [Li58], for example, and Sect. 20.8). It must be realized that this method will not give accurate results if used in the transition region of the convection zone. Baker [Ba63,64b] has computed departures from isentropy in convective envelopes on the basis of the mixing-length theory. As we shall see in the next subsection (Sect. 20.6b), the existence of these zones of hydrogen and helium ionization greatly increases the depths of convective envelopes over those which would otherwise obtain and greatly increases the luminosity of completely convective stars (*cf.* Sect. 23.5).

We note from (20.81) that if Γ_2 is approximately constant, convective stellar envelopes have an approximately *polytropic* structure below the transition region, just as radiative envelopes should have an approximately polytropic structure below the region of hydrogen ionization. The important difference between the two cases, however, is that in the case of radiative envelopes the value of the constant K is simply and directly determined (*cf.* (20.34)) from L and M and the theory of radiative transfer, but *not* by the surface boundary conditions; whereas the value of K in the case of convective transfer is determined from L, M, and R *by* the surface boundary conditions and a complicated and very uncertain theory of convective transfer.

20.6b Structure of Convective Envelopes

Before considering the details of the structure of a convective envelope, let us first consider, for orientation, the structure of the envelope of a star with

$$7500 < T_e(^\circ\mathrm{K}) < 10{,}000.$$

In such a star convection will not be effective in the envelope (*cf.* Sect. 20.5) and we accordingly ignore convection altogether and assume pure radiative transfer in the envelope. The upper limit to T_e is imposed so that hydrogen will not be completely ionized at the photosphere. We shall refer in the following discussion to Figs. 20.3 and 20.4, which show, schematically, temperature T vs. pressure P in the envelope and also $\nabla_r = (\mathrm{d} \ln T/\mathrm{d} \ln P)_{\mathrm{rad}}$,

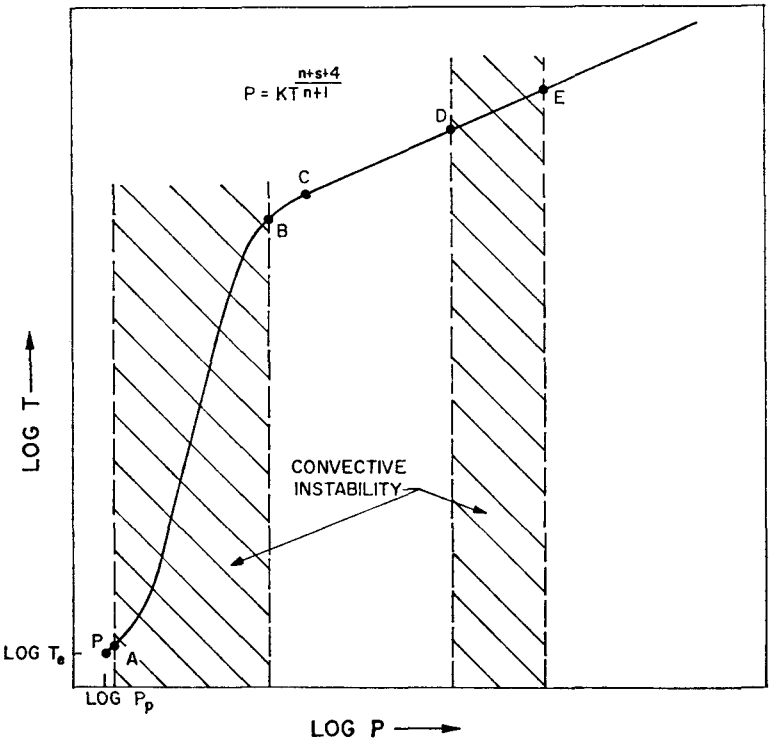

Fig. 20.3 Schematic curve of log T vs. log P in a radiative envelope in a star with $7500 < T_e(°\mathrm{K}) < 10{,}000$.

the "fictitious radiative gradient" (equal to the actual gradient, ∇, in the case of pure radiative transfer), vs. P. The numbers on the vertical scale in Fig. 20.4 are inserted merely to give a rough idea of the scale of the variations in ∇_r; a realistic ∇_r curve might differ considerably, quantitatively, from the one shown.

The point P in Figs. 20.3 and 20.4 represents the photosphere ($\tau = (2/3)$), where $T = T_e$ and $P = P_p \simeq g_s/\kappa_p$ (see (20.16)), where g_s denotes surface gravity and κ_p denotes the photospheric value of the opacity κ. Proceeding inward from P, the point A is the point at which the material first becomes

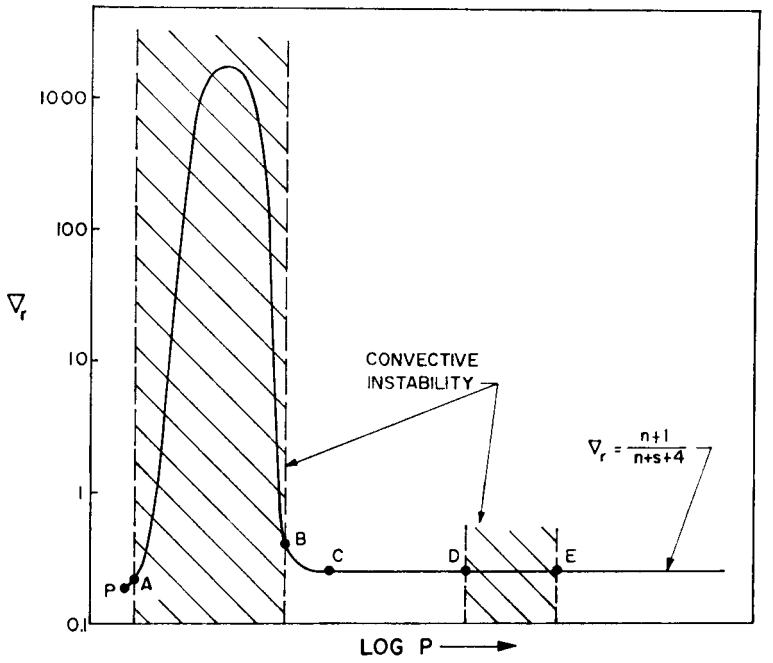

Fig. 20.4 Schematic curve of $\nabla_r \equiv (\mathrm{d}\log T/\mathrm{d}\log P)_{\mathrm{rad}}$ vs. $\log P$ in a radiative envelope in a star with $7500 < T_e(°\mathrm{K}) < 10{,}000$.

unstable against convection, and the region AB is the region of violent convective instability, resulting from the rapid inward increase in κ. We assume that in this region AB the opacity may be represented adequately by the interpolation formula

$$\kappa_{AB} = \kappa_0'' P^{n'} T^{-n'-s'}, \tag{20.84}$$

where we assume, further, that $n'+s'+4<0$. We then have that, if the transfer in this region is purely by radiation (see (20.37), (20.41)),

$$P_{AB} = \left\{ \frac{n'+1}{|n'+s'+4|} \cdot \frac{16}{3} \cdot \frac{g_s}{\kappa_0''} \cdot \frac{1}{T_e^{|n'+s'|}} \left[(2)^{|n'+s'+4|/4} - \left(\frac{T_e}{T} \right)^{|n'+s'+4|} \right] \right\}^{\frac{1}{n'+1}}, \tag{20.85}$$

$$\nabla_r^{(AB)} = \frac{n'+1}{|n'+s'+4|} \left[\left(\frac{2^{1/4} T}{T_e} \right)^{|n'+s'+4|} - 1 \right], \tag{20.86}$$

which show that T increases inward rapidly with increasing P and that, therefore, the gradient ∇_r may become extremely large in this region, as we have seen.

Suppose now that near point B the opacity law switches abruptly to the law

$$\kappa = \kappa_0' P^n T^{-n-s}, \tag{20.87}$$

where now we assume that $n+s+4>0$ (typical values would be $n\simeq 1$, $s\simeq 3$), but that κ is continuous at B. Since (see (20.22)) $\nabla_r \propto \kappa P/T^4$ in regions where $M_r \simeq M$ and $L_r \simeq L$, we have, using (20.87) and the continuity of κ at B, for $T>T_B$ and $P>P_B$:

$$\nabla_r = \nabla_r^{(B)} \left(\frac{P}{P_B}\right)^{n+1} \left(\frac{T}{T_B}\right)^{-n-s-4}, \tag{20.88}$$

where

$$\nabla_r^{(B)} = \frac{3}{16} \cdot \frac{T_e^4}{g_s} \cdot \frac{\kappa_B P_B}{T_B^4} \tag{20.89}$$

is the value of ∇_r at B. It is now easy to show from some of the formulae given in Sect. 20.2 that for pure radiative transfer, by the time T has risen to such a value that $(T/T_B)^{n+s+4} \gg 1$ (*i.e.*, $T>T_C$, where T_C is a few times T_B), ∇_r will have approached the "radiative zero" value:

$$\nabla_r = \frac{n+1}{n+s+4} \qquad (\simeq 0.25 \text{ for } n\simeq 1, s\simeq 3), \tag{20.90}$$

and will retain this value throughout the envelope. The gradient will be stable against convection for $T>T_B$, except possibly in the region DE, where He^+ ionization may lower the value of ∇_{ad} or of s and produce convective instability. Because of the (slight) effect of He^+ ionization on the values of n and s (see Fig. 16.5), the ∇_r curve in Fig. 20.4, if realistically drawn, would probably show some small wiggles in this region.

The region of partial hydrogen ionization will probably be confined to the region AB (*i.e.*, hydrogen is likely to be largely ionized at B). This region is quite thin because of the rapid increase of T with increasing P. Also, any existing convection will not be effective in this region because the rapid rise in T implies low pressures and hence low densitites, which in turn imply small convective efficiency in this region (*cf.* (20.71)). This steep temperature rise also helps make any convection in the He^+ ionization zone ineffective because the pressures (and hence the densitites) for given temperature here are smaller than would otherwise have been the case. Thus, for hot stars such as the kind we are considering here, convection is confined to *thin, ineffective* regions (the region in which hydrogen and first helium ionization occurs, and possibly the region in which second helium ionization occurs).

We consider now the structure of the envelope of a star with, say, $T_e<7500°K$, which is cool enough so that it has an effective and possibly extended convection zone beneath its photosphere. Here we assume that as

we move inward from the photosphere, we reach a temperature within a convection zone, say T_B, where the pressure and density are sufficiently great that convection is effective at temperatures higher than T_B. We also assume that T_B is sufficiently low that hydrogen ionization is not very far advanced here. This assumption follows from the discussion in Sect. 20.4 which illustrates how for cool stars the effect of photo-dissociation of the H^- ion upon the opacity is sufficient to make the radiative gradient ∇_r become a rapidly increasing function of temperature, thus allowing for the possibility of convection ($\nabla_r > \nabla_{ad}$) in regions still too cool for appreciable hydrogen ionization. Finally, we assume for simplicity that the convection is so efficient for $T > T_B$ that the superadiabaticity of the actual gradient ∇ can be neglected, so that we

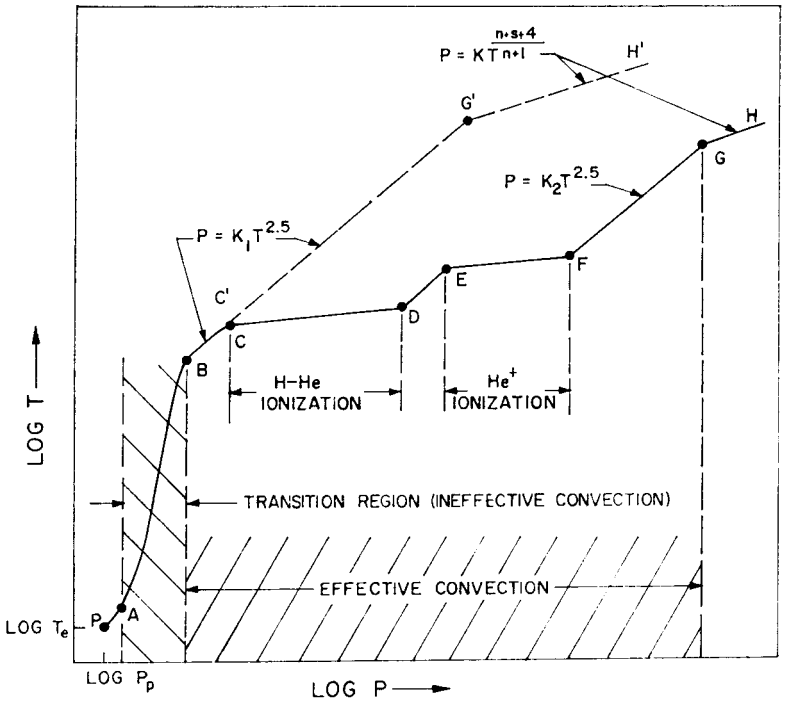

Fig. 20.5 Schematic curve of log T vs. log P in a convective envelope in a star with $T_e < 7500°K$.

can set ∇ equal to the adiabatic gradient ∇_{ad}; in other words, we assume that the P-T relation in the convection zone (for $T > T_B$) is the adiabatic one. We shall refer in the discussion to Figs. 20.5 and 20.6, which show, schematically, log T vs. log P in the envelope and ∇_r, the "fictitious radiative gradient" (now

not equal to ∇), vs. log P (again the numbers on the vertical scale in Fig. 20.6 are inserted only to give a rough indication of relative values; the curve drawn is purely schematic and not quantitatively accurate).

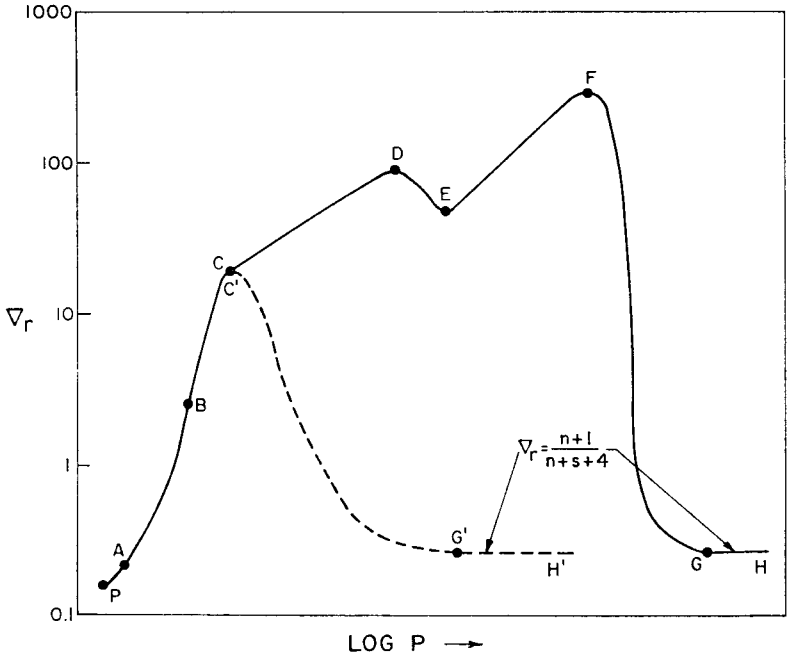

Fig. 20.6 Schematic curve of ∇_r vs. log P in a convective envelope in a star with $T_e < 7500°K$.

Again, point P represents the photosphere and A the point at which instability against convection first sets in ($\nabla_r = \nabla_{ad}$). The region AB is the "transition region", which is convectively unstable and in which radiation and convection compete as transfer mechanisms. Here ∇ lies between ∇_r and ∇_{ad}; ∇ lies closer to ∇_r in regions near A, and closer to ∇_{ad} in regions near B. The structure of this region AB will depend sensitively on the particular theory of convection which is being used; accordingly, there is considerable uncertainty about the precise structure of this region. At B convection becomes effective, so that we may set $\nabla \simeq \nabla_{ad}$. We assume that hydrogen ionization is not very far advanced for $T < T_C$ (therefore $\Gamma_2 \simeq (5/3)$); we accordingly have in the convective region BC (see (20.83))

$$P^{(BC)} = K_1 T^{2.5}, \tag{20.91}$$

where $K_1 = P_B/T_B{}^{2.5}$ is evaluated, in principle at least, from the values of P and T at B (bottom of the transition region). In reality, hydrogen will

probably be partially ionized in region *BC*, so that a more complicated relation between P and T in this region would be required; however, for heuristic reasons, we nevertheless adopt (20.91) in this region.

The fictitious radiative gradient, ∇_r, cannot be evaluated accurately in region *AB*, as a theory of convection must actually be used. If, however, the convection is so inefficient here that $\nabla \simeq \nabla_r$, then ∇_r would be given approximately by (20.86) if $n'+s'+4<0$ or by (20.39) if $n'+s'+4>0$. Assuming the same opacity law $\kappa \propto P^{n'}T^{-n'-s'}$ to apply in region *BC* as in region *AB*, we have in region *BC*

$$\nabla_r^{(BC)} = \nabla_r^{(B)} \left(\frac{P}{P_B}\right)^{n'+1} \left(\frac{T}{T_B}\right)^{-n'-s'-4}, \tag{20.92}$$

where $\nabla_r^{(B)}$ is the value of ∇_r at B. Since (20.91) is assumed to be valid in region *BC*, we have in this region

$$\nabla_r^{(BC)} = \nabla_r^{(B)} \left(\frac{T}{T_B}\right)^{1.5(n'-1)-s'}. \tag{20.93}$$

Since $s'<0$ and $n' \simeq 1$ in region *BC*, it follows that ∇_r continues to increase in this region; *i.e.*, the material becomes more and more convectively unstable as point *C* is approached.

We consider now region *CF*, which contains the zones of hydrogen (H), first helium (He), and second helium (He^+) ionization. Although the H-He and the He^+ ionization zones are usually distinct and well separated in actual stars (as shown schematically in Fig. 20.5), we shall treat these zones for simplicity as only one extensive ionization zone. We shall also assume that $\nabla = \nabla_{ad}$ throughout the regions *CF* and *FG*. Here we need the integrated adiabatic relation between P and T in an ionization zone (see Sect. 20.8). Let us just recall first, however, that $\Gamma_2 \to 1$ and $\Gamma_2/(\Gamma_2-1)$ becomes very large in an ionization region of an abundant element (*cf.* Sect. 9.18). As a very crude approximation, we might replace $\Gamma_2/(\Gamma_2-1)$ in region *CF* by a constant average value $\langle \Gamma_2/(\Gamma_2-1) \rangle$, so that, approximately

$$P \propto T^{\langle \Gamma_2/(\Gamma_2-1) \rangle} \tag{20.94}$$

in region *CF*. Since $\langle \Gamma_2/(\Gamma_2-1) \rangle$ is a fairly large number, it follows that P increases very rapidly inward with increasing T, *i.e.*, T increases very *slowly* with increasing P (which is just the opposite of the behavior for radiative transport in an ionization zone). At the bottom of the ionization region (point *F*), then, the pressure is very large for the temperature, much larger than if the ionization regions had been neglected. We note also that because of the small average temperature gradient in region *CF*, the ionization regions are considerably "drawn out" and spread over a large portion of the

envelope; this is in marked contrast to the situation in radiative envelopes, where because of the steep temperature gradient the ionization zones are very thin. In the region FG, below the ionization zones, Γ_2 is again essentially constant and approximately equal to (5/3), so that here

$$P^{(FG)} = K_2 T^{2.5}, \tag{20.95}$$

where the value of K_2 is determined by the value of K_1 (see next paragraph).

From Sect. 20.8 we have the following result, based on the constancy of the entropy along an adiabat, for a "classical" perfect gas consisting only of hydrogen and helium: If hydrogen and helium are essentially unionized at point C and essentially completely ionized at point F (including both stages of helium ionization), we have as the relation between the values of the quantity $(P/T^{5/2})$ at points C and F:

$$\left(\frac{P}{T^{5/2}}\right)_F = C \cdot \left(\frac{P}{T^{5/2}}\right)_C^{\alpha}, \tag{20.96}$$

where the values of the constants C and α depend on the helium/hydrogen ratio B (by numbers):

$$\alpha \equiv \frac{1+B}{2+3B}, \tag{20.97}$$

$$C \equiv e^{(5/2)(1-\alpha)} \cdot \frac{1}{\alpha} \cdot \left(\frac{1+B}{1+2B}\right)^{1-\alpha} \cdot 2^{\alpha[2B/(1+B)]} \cdot \left[\frac{(2\pi m_e)^{3/2} k^{5/2}}{h^3}\right]^{1-\alpha} \tag{20.98}$$

$$= 10^{0.6085(1-\alpha)} \frac{2^{2(1-2\alpha)}}{\alpha^{\alpha}(1-\alpha)^{1-\alpha}}. \tag{20.99}$$

Here m_e, k, and h denote, respectively, the electron rest mass, the Boltzmann constant, and Planck's constant; and c.g.s. units are used in (20.99). Using (20.91) and (20.95), we may also write (20.96) in the form

$$K_2 = C \cdot K_1^{\alpha}, \tag{20.100}$$

which is the relation between the K's above and below the ionization region. For $B = 0$ (pure hydrogen), we have

$$\alpha = 1/2,$$

$$C = 2e^{5/4}\left[\frac{(2\pi m_e)^{3/2} k^{5/2}}{h^3}\right]^{1/2} = 4.03,$$

so that

$$K_2 \simeq 4.0 K_1^{1/2} \qquad \text{(pure hydrogen)}. \tag{20.101}$$

For $B = \infty$ (pure helium), we have

$$\alpha = (1/3),$$

$$C = 3e^{5/3}\left[\frac{(2\pi m_e)^{3/2}k^{5/2}}{h^3}\right]^{2/3} = 7.63,$$

so that

$$K_2 \simeq 7.6K_1^{1/3} \qquad \text{(pure helium)}. \tag{20.102}$$

Since a typical value of K_1 might be $\sim 10^{-5}$ c.g.s. units,* we see (assuming pure hydrogen) that $K_2 \sim 10^{-2}$, *i.e.*, that $K_2/K_1 \sim 10^3$. Hence the pressure at a given temperature below the ionization region can perhaps be some 10^3 times greater than would have been the case if the effects of the ionization zones had been ignored.

In Fig. 20.5 the dashed line $C'G'H'$ shows the T vs. P curve that would have been obtained if the ionization regions had been ignored.

What determines the depth of the convective envelope, *i.e.*, the point at which ∇_r has decreased in value until it is again equal to ∇_{ad}? It is clear that to answer this question, we must consider the behavior of ∇_r throughout the convection zone.

We have already followed the course of ∇_r down to the point C, where hydrogen ionization is assumed to set in. Previous discussion has shown that the opacity $\kappa \propto P^n T^{-n-s}$ is a strongly increasing function of T in regions where H is only partially ionized (assuming H to be the most abundant element), *i.e.*, that s is fairly large and negative in such regions. Since H will become nearly fully ionized somewhere between points C and D, we may expect the opacity law to change into a "Kramer's" type of law somewhere between C and D. We shall assume for simplicity that the opacity law switches abruptly at point C to the law $\kappa \propto P^n T^{-n-s}$, where now $n+s+4>0$ (say $n \simeq 1, s \simeq 3$), and κ is continuous at C. We then have for $T \geq T_C$

$$\nabla_r = \nabla_r^{(C)}\left(\frac{P}{P_C}\right)^{n+1}\left(\frac{T}{T_C}\right)^{-n-s-4}, \tag{20.103}$$

where the sub- and superscripts C refer to values at point C.

The $P(T)$ relation is extremely complicated, quantitatively, in region CF (see Sect. 20.8), and so also is the detailed behavior of ∇_r in this region. However, the qualitative features of the ∇_r curve in region CF (see Fig. 20.6) are easily understood from (20.103) (recalling that $n+s+4>0$) by noting

* For example, for the sun we may estimate the value of K_1 by using the relation $K_1 = P_p/T_e^{2.5}$, where P_p and T_e are photospheric values of P and T. Taking $P_p \sim 10^5$ dynes/cm^2 and $T_e \sim 6\times 10^3$ °K, we obtain $K_1 \sim 3\times 10^{-5}$.

that T is nearly constant in regions CD and EF and that $P \propto T^{2.5}$ in region DE. Hence ∇_r should increase inward in both regions CD and EF. Quantitatively, we know at least the relation between the value of the quantity $(P/T^{2.5})$ at points just above C (where hydrogen and helium are essentially unionized) and that at points just below F (where hydrogen and helium are essentially completely ionized). Using (20.91) and (20.95) in (20.103), we obtain in region FG

$$\nabla_r^{(FG)} = \nabla_r^{(C)} \left(\frac{K_2}{K_1}\right)^{n+1} \left(\frac{T}{T_C}\right)^{1.5(n-1)-s} \tag{20.104}$$

$$= \nabla_r^{(F)} \left(\frac{T}{T_F}\right)^{1.5(n-1)-s}, \tag{20.105}$$

where

$$\nabla_r^{(F)} = \nabla_r^{(C)} \cdot \left(\frac{K_2}{K_1}\right)^{n+1} \left(\frac{T_F}{T_C}\right)^{1.5(n-1)-s} \tag{20.106}$$

is the value of ∇_r at some point just below F. We note that since $n \simeq 1$ and $K_2/K_1 \gg 1$, the factors in (20.104) and (20.106) containing the K's may be quite large, perhaps as large as $10^5 - 10^6$, say. On the other hand, since $s \simeq 3$ and $T_F/T_C \sim 4-5$, say, the factor containing the T's in (20.106) is likely to be of order 10^{-2}. Hence the factor multiplying $\nabla_r^{(C)}$ in (20.106) is still large compared to unity, say perhaps 10^3–10^4. This means that the value of ∇_r has been increased by a large factor in going down through the ionization zones of hydrogen and helium; the material is consequently considerably more unstable against convection at F than it was at C.

At points *interior* to the ionization zones ($T > T_F$), where $P = K_2 T^{2.5}$, (20.105) shows that, since $n \simeq 1$ and $s \simeq 3$, ∇_r varies approximately as T^{-3}, so that ∇_r now steadily diminishes in value as greater and greater depths below the ionization zones are attained. When ∇_r has fallen to the value $\nabla_{ad} = 0.4$ (if $\Gamma_2 = (5/3)$), we again have stability against convection, and it is at this point (point G in Figs. 20.5 and 20.6) that the convection zone ends. For $T > T_G$, radiative transfer will obtain (at least in the envelope). In fact, at depths for which T is somewhat larger than T_G, the radiative zero solution, for which $\nabla_r = (n+1)/(n+s+4)$, will have been reached, provided that M_r and L_r are still approximately equal to M and L (this may not be the case at all in sufficiently cool stars).

It is clear from these considerations that the larger is the value of $\nabla_r^{(F)}$, the deeper the convective envelope will be. If we had not taken the ionization zones of hydrogen and helium into account (see dashed curves in Figs. 20.5 and 20.6), the points F and C would have coincided and we would have had $K_2/K_1 = 1$ and $T_F = T_C$. Hence $\nabla_r^{(F)}$ would have had the much smaller

value $\nabla_r^{(C)}$, and it is clear that the convective envelope would have been much shallower in this case than in the former one. Briefly stated, we may say that the ionization zones hold the temperature down in these zones, making them almost isothermal; whereas the pressure continues to increase inward through these zones. Immediately beneath these zones, then, the pressure is very large for the temperature, and the fictitious radiative gradient $\nabla_r \propto \kappa P/T^4$ is very large, thus making the material highly unstable against convection here. We conclude that the presence of the hydrogen and helium ionization zones considerably deepens the convective envelopes of cooler stars over the depths they would otherwise have.

We consider now the dependence of the depth of the convective envelope on T_e. We combine (20.106), (20.100), (20.93), (20.91), (20.24b), (20.23) and (20.22) to obtain

$$\nabla_r^{(F)} = \frac{3}{16} \cdot \frac{T_e^4}{g_s} \kappa_0' C^{n+1} K_1^{n'+1-(1-\alpha)(n+1)} T_C^{1.5(n'-n)+s-s'} \cdot T_F^{1.5(n-1)-s}, \tag{20.107}$$

where (20.24b) is applied at point B, and where primed n and s denote values *above* point C, unprimed n and s denote values *below* point C. Since $n \simeq n' \simeq 1$ and $\alpha \simeq (1/2)$ (for a mixture composed predominantly of hydrogen), the exponent of K_1 is approximately unity so that $\nabla_r^{(F)}$ increases with increasing K_1. Since in our simplified picture the value of the constant K_1 is determined by the values of P and T at the point B (see Fig. 20.5), we see that the larger is P_B and the smaller is T_B, the greater is K_1 and hence also $\nabla_r^{(F)}$. In order to consider the dependence of $\nabla_r^{(F)}$ (which controls the depth of the convection zone) on T_e, we must consider the dependence of K_1 on T_e. Since points C and F are defined, respectively, as the points where H ionization is just setting in and where He^+ ionization is essentially complete, it follows that T_C ($\sim 8000-10{,}000\,°K$) and T_F ($\sim 50{,}000\,°K$, say) do not depend sensitively on stellar parameters.

Since a theory of convection is actually required in order to evaluate K_1, our considerations will be quite uncertain quantitatively. Let us, for the sake of simplicity, assume that the energy transfer in region AB is purely radiative (this will probably cause the value of K_1 to be underestimated, but this is of no consequence in our present considerations). We then have for T_B a few times T_e (*cf.* (20.35), (20.37)), approximately,

$$P_B \propto T_B^x \frac{g_s^{\frac{1}{n'+1}}}{T_e^y} \tag{20.108a}$$

and

$$K_1 \propto T_B^{x-2.5} \frac{g_s^{\frac{1}{n'+1}}}{T_e^y}, \tag{20.108b}$$

where

$$x = \frac{n'+s'+4}{n'+1}, \quad y = \frac{4}{n'+1} \quad \text{for } n'+s'+4>0,$$

$$x = 0, \quad y = \frac{|n'+s'|}{n'+1} \quad \text{for } n'+s'+4<0.$$

Equation (20.107) then becomes (considering T_C and T_F as fixed)

$$\nabla_r^{(F)} \propto T_e^{4-y[n'+1-(1-\alpha)(n+1)]} \cdot \frac{1}{g_s^{1-\{[n'+1-(1-\alpha)(n+1)]/(n+1)\}}}$$

$$\frac{1}{T_B^{(2.5-x)[n'+1-(1-\alpha)(n+1)]}}. \tag{20.108c}$$

Taking the typical values $n' \simeq n \simeq 1$, $\alpha \simeq (1/2)$, we have

$$\nabla_r^{(F)} \propto \frac{T_e^{4-y}}{g_s^{1/2} T_B^{2.5-x}}. \tag{20.108d}$$

For $T_B > 5040\,^\circ\mathrm{K}$, we have seen that a representative value is $s' = -10$, which gives $x = 0$, $y = 4.5$, and

$$\nabla_r^{(F)} \propto \frac{1}{g_s^{1/2} T_e^{1/2} T_B^{2.5}}. \tag{20.108e}$$

Since T_G (temperature at bottom of convection zone) $\propto [\nabla_r^{(F)}]^{1/3}$ (*cf.* (20.105)), we have also

$$T_G \propto \frac{1}{g_s^{1/6} T_e^{1/6} T_B^{5/6}} \qquad (T_B > 5040\,^\circ\mathrm{K}). \tag{20.108f}$$

For $T_B < 5040\,^\circ\mathrm{K}$ we have $s' \simeq -3$, whence $x = 1$, $y = 2$, and

$$\nabla_r^{(F)} \propto \frac{T_e^2}{g_s^{1/2} T_B^{1.5}}; \tag{20.108g}$$

also

$$T_G \propto \frac{T_e^{2/3}}{g_s^{1/6} T_B^{1/2}} \qquad (T_B < 5040\,^\circ\mathrm{K}). \tag{20.108h}$$

It is probable that as density and pressure in the sub-photospheric regions increase in cooler and cooler stars, the temperature T_B at which convection

becomes effective also is likely to be smaller in cooler stars (as is confirmed by detailed calculations of Vardya [Va60b,64]). It may, in fact, be the case that the ratio T_B/T_e is approximately constant (*i.e.*, constant value of optical depth at the point where convection becomes effective). Hence it is clear from (20.108f) that the temperature at the bottom of the convection zone increases roughly linearly with $1/T_e$, *i.e.*, increases as one goes to cooler and cooler stars, for $T_e > 5040\,°\mathrm{K}$. For $T_e < 5040\,°\mathrm{K}$, (20.108g) suggests that $\nabla_r^{(F)}$ (and also T_G) *decreases* slowly with decreasing T_e. The calculations of Baker [Ba63,64b] also show that the temperature T_G at the bottom of the convection zone tends to level off and perhaps even shows signs of decreasing with decreasing T_e at $T_e \simeq 5100\,°\mathrm{K}$. If T_G remains approximately constant or decreases slightly with decreasing T_e, then a sufficiently cool star could become completely convective only by the central temperature falling to a value near that of T_G. According to Limber [Li58], the late M dwarfs are completely convective (*cf.* Sect. 26.3). Such stars will be discussed in Sect. 23.5.

We emphasize the approximate nature of our considerations. In real stars hydrogen is likely to be partially ionized at point B in Figs. 20.5 and 20.6. If this partial ionization were to be taken into account, the relation between K_1 and K_2 would be considerably more complicated (*cf.* Sect. 20.8) and the depth of the convection zone as calculated above would be reduced somewhat. Also, since the value of K_1 is determined by the values of P and T at the bottom of the "transition region," then the value of K_1 is rendered uncertain by the uncertainties in the theory of convection, which determines the detailed structure of this region. Also, the assumption that the opacity law is Kramers-like below point C ($n \simeq 1$, $s \simeq 3$, n, s constant below point C) introduces error because H is not fully ionized at point C. Finally, the procedure of setting $\nabla = \nabla_{ad}$ introduces some error, which is the less serious, the lower is T_e. Baker [Ba63,64b] has shown that the entropy actually increases somewhat in traversing the convection zone from top to bottom, which results in a slightly smaller depth of the convection zone than would be obtained by setting $\nabla = \nabla_{ad}$. This is to be expected since, actually, $\nabla > \nabla_{ad}$, which means that the actual temperature at a given pressure P is somewhat larger than would be given by setting $\nabla = \nabla_{ad}$, and hence that the actual entropy increases inward in a convection zone (see also (13.31)). The uncertainty in the value of K_1, however, is more serious than the non-adiabaticity of the convection zone, since the value of K_1 determines *which* adiabat applies to the adiabatic region of the convection zone. In spite of these possible complications, our simple picture is nevertheless qualitatively correct.

It is important to note that careful attention to the surface boundary conditions is absolutely essential to obtain realistic results for main sequence

stars cooler than about 7000 °K; as we have seen, in these cases the structure of the entire outer portions of the star depends critically on these boundary conditions. If we had ignored them, the existence of deep convective envelopes in cool stars might have been missed altogether (indeed, this was the case prior to Osterbrock's now classic work [Os53]). In hot stars such careful attention is not needed (*cf.* Sect. 20.3); indeed, the simple "radiative zero" boundary conditions can generally be used.

Finally, we note that, if the envelope of a late type star contains strong magnetic fields which may strongly affect (if not impede) convective motions, then the structure of such an envelope may be quite different from the structure that we have described above.

20.7 Temperature Distribution in the Envelope

In general, it is not possible to obtain simple analytic expressions for the distribution of temperature with depth in an envelope. In the case of radiative envelopes the reason is primarily the complicated behavior of the opacity in the regions in and above the level of hydrogen ionization. In the case of convective envelopes the reason is primarily the existence of the "transition region" where a theory of convection should be used. We showed, however, that in the case of both radiative and convective envelopes the deeper regions tend to take on an approximately polytropic structure; *i.e.*, in such regions we have, approximately,

$$P = KT^{n_e+1}, \tag{20.109}$$

where

$$n_e = \begin{cases} \dfrac{s+3}{n+1} & \text{(radiative envelopes)} \\ \dfrac{1}{\Gamma_2 - 1} & \text{(convective envelopes)} \end{cases} \tag{20.110a,b}$$

and

$$K = \begin{cases} \left[\dfrac{n+1}{n+s+4} \cdot \dfrac{16\pi acGM}{3\kappa_0' L}\right]^{\frac{1}{n+1}} & \text{(radiative envelopes)} \\ K(L, M, R, \text{comp.}) & \text{(convective envelopes)}, \end{cases} \tag{20.111a,b}$$

provided that n_e and K are constant. In (20.111b) K is evaluated from the surface boundary conditions (except possibly in the case of completely convective stars).

If we neglect the complicated structure of the outermost layers and simply assume that (20.109) may be used as an adequate approximation throughout the envelope, then a simple analytic formula for the temperature distribution

in the envelope can be obtained. First, however, we formulate the problem more generally.

We write the equation of hydrostatic equilibrium in the form

$$\frac{dP}{dr}=P\frac{d\ln P}{d\ln T}\cdot\frac{1}{T}\frac{dT}{dr}=-G\frac{M_r}{r^2}\rho, \tag{20.112}$$

which gives, using the definition $n_e+1 = d\ln P/d\ln T$ of effective polytropic index,

$$(n_e+1)\frac{dT}{dr}=-G\frac{M_r}{r^2}\cdot\rho\frac{T}{P} \tag{20.113}$$

$$=-\frac{\beta\mu GM_r}{\mathscr{R}}\cdot\frac{1}{r^2}, \tag{20.114}$$

where we have used the "perfect" gas equation of state (20.67) (with radiation pressure included) in (20.113) to obtain (20.114). Assuming that $(\beta\mu)$ is constant in the envelope and that $M_r\approx M$, we obtain from (20.114)

$$\int_{T_e}^{T}(n_e+1)dT'=\frac{\beta\mu GM}{\mathscr{R}}\left(\frac{1}{r}-\frac{1}{R}\right), \tag{20.114'}$$

where we have taken $T = T_e$ (effective temperature) at $r = R$ (photospheric radius).

If (n_e+1) is constant throughout the relevant regions of the envelope (as in (20.110)), then we obtain from (20.114'), neglecting T_e in comparison to T, the simple analytic solution referred to above:

$$T=\frac{1}{n_e+1}\cdot\frac{\beta\mu GM}{\mathscr{R}}\cdot\left(\frac{1}{r}-\frac{1}{R}\right)$$

$$=\frac{1}{n_e+1}\left(\frac{G}{\mathscr{R}}\right)\cdot\left(\frac{\beta\mu M}{R}\right)\cdot\left(\frac{1}{x}-1\right), \tag{20.115}$$

where $x\equiv r/R$. If M and R are expressed in solar units, we have

$$T=\frac{22.91\times10^6}{n_e+1}\cdot\frac{\beta\mu M}{R}\left(\frac{1}{x}-1\right)\text{°K}. \tag{20.116}$$

We note that to the approximation to which we are working, (20.115) applies to either radiative or convective envelopes since both obey the same type of polytropic equation (20.109). The only difference between the two types of envelope, from the standpoint of (20.115), is that n_e will have one value ($\simeq 3$) for radiative envelopes and another value ($\simeq 1.5$) for convective envelopes.

20.8 Integrated Adiabats in Hydrogen and Helium Ionization Zones

It was stated in Sect. 20.6 that if $\Gamma_2 = const.$ in a convection zone in a star, then the integrated adiabats are simply

$$P = KT^{\Gamma_2/(\Gamma_2-1)} \tag{20.117a}$$

$$= KT^{2.5} \quad \text{if} \quad \Gamma_2 = (5/3), \tag{20.117b}$$

where K serves to identify the particular adiabat under consideration. It was also stated there that even if Γ_2 is not constant (as in an ionization zone of a dominant element, *cf.* Sect. 9.18), it is still possible, by assuming the local specific entropy S to remain constant along an adiabat, to write down analytic expressions for the integrated adiabats. We shall obtain such expressions in this section for a gaseous mixture of H and He undergoing ionization. Equivalent expressions have also been derived by Limber [Li58]. Applications of these expressions are made in Sects. 20.6 and 23.5.

(It is also possible to obtain integrated adiabats directly by numerically integrating the equation

$$\left(\frac{d\ln P}{d\ln T}\right)_S = \frac{\Gamma_2}{\Gamma_2 - 1} \equiv f(P,T) \tag{20.118}$$

from some initial pair of values of P and T which serves to identify the particular adiabat under consideration. Examples of formulae for computing Γ_2 are found in Chap. 9. Such integrated adiabats have been computed by Vardya [Va60a,65]).

We consider a mixture of non-interacting, non-relativistic, Maxwell-Boltzmann gases in thermodynamic equilibrium, all having the same temperature T, and we neglect radiation pressure. Each stage of ionization of each species of particle is treated as a distinct kind of particle, as are also the free electrons. Assuming the electrons to be Maxwell-Boltzmann particles means, of course, that the electron gas is being assumed non-degenerate (*cf.* Chaps. 3 and 10). If n_i denotes the number density of particles of type i, each of (rest) mass m_i, we have for the entropy per unit volume contributed by particles of type i, ignoring the excitation energy in the case of "compound" particles (see (10.68a)),

$$S_i = kn_i \ln\left[\frac{T^{5/2}}{P_i} \cdot \frac{B_i(T)(2\pi m_i)^{3/2}k^{5/2}e^{5/2}}{h^3}\right], \tag{20.119}$$

where $P_i = n_i kT$ is the partial pressure exerted by i-type particles, $B_i(T)$ is the partition function for particles of type i (see (3.25)), k is Boltzmann's

constant, h is Planck's constant, and e is the base of the natural logarithms. We now use the relation $P_i = (n_i/n)P$ in (20.119), where $n = \sum_i n_i$ is the total particle number density and $P = \sum_i P_i$ is the total pressure in the system. We then form the sum $S = \sum_i S_i$ over all types of particle present and divide through by ρ, the mass density of the mixture, so as to obtain the total *specific* entropy $s \equiv S/\rho$ (entropy per unit mass). Making use of the relation $n/\rho = N_0/\mu$, where N_0 is Avogadro's number and μ is the mean molecular weight (*cf.* Chap. 15), and dividing the resulting equation through by $N_0 k$, we obtain for the total specific entropy in units of $N_0 k$

$$\frac{s}{N_0 k} = \frac{1}{\mu} \sum_i \frac{n_i}{n} \ln \left[\frac{T^{5/2}}{P} \cdot \frac{n}{n_i} \cdot \frac{B_i(T)(2\pi m_i)^{3/2} k^{5/2} e^{5/2}}{h^3} \right]. \tag{20.120}$$

We now apply (20.120) to a mixture consisting only of H^0 (unionized hydrogen), H^+ (ionized hydrogen), He^0 (unionized helium), He^+ (singly ionized helium), He^{++} (doubly ionized helium), and free electrons, and we assume that the free electrons have all come from the ionization of H and He. This assumption will be adequately realized for a "normal" composition (predominantly H), even if some metals are present, for temperatures $\gtrsim 5000\,°\mathrm{K}$, for then the number of electrons supplied by ionization of metals will form only a small fraction of the number supplied by hydrogen ionization (*cf.* Sect. 20.4). We now write in an obvious notation

$$n_{\mathrm{H}} \equiv n(\mathrm{H}^0) + n(\mathrm{H}^+), \tag{20.121}$$

$$n_{\mathrm{He}} \equiv n(\mathrm{He}^0) + n(\mathrm{He}^+) + n(\mathrm{He}^{++}), \tag{20.122}$$

where n_{H} and n_{He} are the total number densities of atoms and ions of, respectively, H and He. Letting n_e denote the electron number density, we have

$$n = n_{\mathrm{H}} + n_{\mathrm{He}} + n_e \tag{20.123}$$

as the total particle number density in the mixture. We now define

$$B \equiv n_{\mathrm{He}}/n_{\mathrm{H}} \tag{20.124}$$

as the He/H abundance ratio (by numbers) and

$$\begin{aligned} x &\equiv \text{fraction of all H atoms and ions that are (once) ionized,} \\ y_1 &\equiv \text{fraction of all He atoms and ions that are once ionized,} \\ y_2 &\equiv \text{fraction of all He atoms and ions that are twice ionized.} \end{aligned} \tag{20.125}$$

The following relations are then immediately obtained:

$$n_e = x n_{\mathrm{H}} + (y_1 + 2y_2) n_{\mathrm{He}} = n_{\mathrm{H}}[x + (y_1 + 2y_2)B], \tag{20.126}$$

$$n = (1+x) n_{\mathrm{H}} + (1 + y_1 + 2y_2) n_{\mathrm{He}} = n_{\mathrm{H}}[1 + x + (1 + y_1 + 2y_2)B], \tag{20.127}$$

$$\frac{n(\mathrm{H}^0)}{n} = \frac{1-x}{1+x+B(1+y_1+2y_2)}, \quad \frac{n(\mathrm{H}^+)}{n} = \frac{x}{1+x+B(1+y_1+2y_2)},$$

$$\frac{n(\mathrm{He}^0)}{n} = \frac{(1-y_1-y_2)B}{1+x+B(1+y_1+2y_2)}, \quad \frac{n(\mathrm{He}^+)}{n} = \frac{y_1 B}{1+x+B(1+y_1+2y_2)}, \tag{20.128}$$

$$\frac{n(\mathrm{He}^{++})}{n} = \frac{y_2 B}{1+x+B(1+y_1+2y_2)}, \quad \frac{n_e}{n} = \frac{x + B(y_1+2y_2)}{1+x+B(1+y_1+2y_2)}.$$

Moreover, taking the atomic masses (in A.M.U.'s) of H and He to be 1 and 4, respectively, we have for the mean molecular weight of the mixture (ignoring elements heavier than He^4)

$$\mu \simeq \frac{n_{\mathrm{H}} + 4n_{\mathrm{He}}}{n} = \frac{1+4B}{1+x+B(1+y_1+2y_2)}. \tag{20.129}$$

Finally, we assume that the partition functions $B_i(T)$ can be approximated in the case of "compound" particles by their first terms. Including nuclear spins (and assuming the nuclear spin of He^4 to be zero), we have, again in an obvious notation,

$$\begin{aligned} &B(\mathrm{H}^0) = 4, \quad B(\mathrm{H}^+) = 2, \quad B(\mathrm{He}^0) = 1, \\ &B(\mathrm{He}^+) = 2, \quad B(\mathrm{He}^{++}) = 1, \quad B(e) = 2.^* \end{aligned} \tag{20.130}$$

Using (20.128), (20.129), and (20.130) in (20.120), we obtain

$$\begin{aligned} \frac{s}{N_0 k} = \frac{1}{1+4B} \Bigg\{ &(1-x) \ln \left[\frac{T^{5/2}}{P} \cdot \frac{1+x+B(1+y_1+2y_2)}{1-x} \cdot \frac{4(2\pi m_{\mathrm{H}})^{3/2} k^{5/2} e^{5/2}}{h^3} \right] \\ &+ x \ln \left[\frac{T^{5/2}}{P} \cdot \frac{1+x+B(1+y_1+2y_2)}{x} \cdot \frac{2(2\pi m_{\mathrm{H}})^{3/2} k^{5/2} e^{5/2}}{h^3} \right] \\ &+ B(1-y_1-y_2) \ln \left[\frac{T^{5/2}}{P} \cdot \frac{1+x+B(1+y_1+2y_2)}{B(1-y_1-y_2)} \right. \\ &\left. \cdot \frac{(2\pi m_{\mathrm{He}})^{3/2} k^{5/2} e^{5/2}}{h^3} \right] \Bigg\} \end{aligned} \tag{20.131}$$

* The values of the B's for He^0, He^+, and He^{++} in (20.130) are one-half the values as given by Limber [Li58], who incorrectly took the spin of the He^4 nucleus to be (1/2). This factor of two, however, does not affect Limber's conclusions or the final results as expressed in (20.133) and in the formulae in this section following (20.133).

$$
\begin{aligned}
&+y_1 B \ln\left[\frac{T^{5/2}}{P}\cdot\frac{1+x+B(1+y_1+2y_2)}{y_1 B}\cdot\frac{2(2\pi m_{\mathrm{He}})^{3/2}k^{5/2}e^{5/2}}{h^3}\right]\\
&+y_2 B \ln\left[\frac{T^{5/2}}{P}\cdot\frac{1+x+B(1+y_1+2y_2)}{y_2 B}\cdot\frac{(2\pi m_{\mathrm{He}})^{3/2}k^{5/2}e^{5/2}}{h^3}\right]\\
&+[x+B(y_1+2y_2)]\ln\left[\frac{T^{5/2}}{P}\cdot\frac{1+x+B(1+y_1+2y_2)}{x+B(y_1+2y_2)}\right.\\
&\left.\cdot\frac{2(2\pi m_e)^{3/2}k^{5/2}e^{5/2}}{h^3}\right]\Bigg\}\\
=&\frac{1}{1+4B}\Bigg[\Bigg[[1+x+B(1+y_1+2y_2)]\\
&\cdot\ln\left\{\frac{T^{5/2}}{P}[1+x+B(1+y_1+2y_2)]\,e^{5/2}\right\}\\
&-(1-x)\ln(1-x)-x\ln x-B(1-y_1-y_2)\ln[B(1-y_1-y_2)] \qquad (20.132)\\
&-y_1 B\ln(y_1 B)-y_2 B\ln(y_2 B)\\
&-[x+B(y_1+2y_2)]\ln[x+B(y_1+2y_2)]\\
&+\ln\left[\frac{(2\pi m_{\mathrm{H}})^{3/2}k^{5/2}}{h^3}\right]+B\ln\left[\frac{(2\pi m_{\mathrm{He}})^{3/2}k^{5/2}}{h^3}\right]\\
&+[x+B(y_1+2y_2)]\ln\left[\frac{(2\pi m_e)^{3/2}k^{5/2}}{h^3}\right]+[1+B(y_1+y_2)]2\ln 2\Bigg]\Bigg],
\end{aligned}
$$

where m_{H}, m_{He}, and m_e denote, respectively, the H, He, and electron (rest) masses (we neglect the mass differences between ions of a particular atomic species).

Equation (20.132) is the explicit expression of the integrated adiabats for the particular system considered here, where the value of the specific entropy s specifies the particular adiabat under consideration. That (20.132) is indeed the expression for the integrated adiabats can be seen from the fact that the degrees of ionization x, y_1, and y_2 are functions of P and T (*cf.* Chap. 15), so that (20.132) is a one-to-one relation between P and T along an adiabat. For $x = y_1 = y_2 = 0$ (no ionization) and for $x = 1$, $y_1 = 0$, $y_2 = 1$ (complete ionization), (20.132) yields $P/T^{5/2} = const.$, which is just (20.117b).

Equation (20.132) will be simplified if conditions at point A (characterized by values $P^{(A)}$, $T^{(A)}$) along a given adiabat are such that He is largely neutral (*i.e.*, $y_1^{(A)} \simeq y_2^{(A)} \simeq 0$), and if conditions at point B (characterized by values $P^{(B)}$, $T^{(B)}$) along the same adiabat are such that H is almost fully ionized

(*i.e.*, $x^{(B)} \simeq 1$) and such that very little neutral He is left (*i.e.*, $y_1^{(B)} \simeq 1 - y_2^{(B)}$). Evaluating the right side of (20.132) at points A and B and equating (since s is being assumed constant on a given adiabat), we obtain

$$\left(\frac{P}{T^{5/2}}\right)_B = C\left(\frac{P}{T^{5/2}}\right)_A^{\alpha}, \tag{20.133}$$

where

$$\alpha \equiv \frac{1+x^{(A)}+B}{2+B(2+y_2^{(B)})} \tag{20.134}$$

and

$$\begin{aligned}\ln C \equiv\ & (5/2)(1-\alpha)+\ln[2+B(2+y_2)]-\alpha\ln[1+x+B] \\ & +\frac{1}{2+B(2+y_2)}\Big\{(1-x)\ln(1-x)+2x\ln x+B\ln B \\ & -B(1-y_2)\ln[B(1-y_2)] \\ & -By_2\ln(By_2)-[1+B(1+y_2)]\ln[1+B(1+y_2)] \\ & +[1-x+B(1+y_2)]\ln\left[\frac{(2\pi m_e)^{3/2}k^{5/2}}{h^3}\right]+2B\ln 2\Big\}.\end{aligned} \tag{20.135}$$

In (20.135) we have omitted the superscripts (A) and (B), but it is to be understood that x (degree of H ionization) is to be evaluated at point A and y_2 (degree of second He ionization) is to be evaluated at point B. Equation (20.133) gives the value of $(P/T^{5/2})$ at some point in the H or He^+ ionization zones, assuming points A and B to be connected by an adiabat identified by the value of $(P/T^{5/2})$ at point A.

If $y_2^{(B)} \simeq 1$ (essentially complete ionization at point B), we have (20.133) again, with (remembering that $x \equiv x^{(A)}$)

$$\alpha = \frac{1+x+B}{2+3B}, \tag{20.136}$$

$$\begin{aligned}C = & \left[\frac{(2\pi m_e)^{3/2}k^{5/2}e^{5/2}}{h^3}\right]^{1-\alpha}\cdot\frac{(2+3B)^{1-\alpha}}{\alpha^{\alpha}} \\ & \cdot 2^{2B/(2+3B)}\cdot\left[\frac{(1-x)^{1-x}x^{2x}}{(1+2B)^{1+2B}}\right]^{1/(2+3B)},\end{aligned} \tag{20.137}$$

where

$$\left[\frac{(2\pi m_e)^{3/2}k^{5/2}e^{5/2}}{h^3}\right] = 10^{0.6085}\ \text{c.g.s. units}. \tag{20.138}$$

If $y_2^{(B)} \simeq 1$ and $x^{(A)} \simeq 0$ (essentially no ionization at point A and essentially complete ionization at point B), we have (20.133) again, with

$$\alpha = \frac{1+B}{2+3B}, \tag{20.139}$$

$$C = \left[\frac{(2\pi m_e)^{3/2} k^{5/2} e^{5/2}}{h^3}\right]^{1-\alpha} \cdot \frac{1}{\alpha^\alpha (1-\alpha)^{1-\alpha}} \cdot 2^{2(1-2\alpha)}. \tag{20.140}$$

Finally if $x^{(A)} \simeq 1$ (essentially complete H ionization at point A) and $y_2^{(B)} \simeq 1$ (essentially complete H and He ionization at point B), we have (20.133) again, with

$$\alpha = \frac{2+B}{2+3B}, \tag{20.141}$$

$$C = \left[\frac{(2\pi m_e)^{3/2} k^{5/2} e^{5/2}}{h^3}\right]^{1-\alpha} \frac{(2+3B)^{1-\alpha}}{\alpha^\alpha} \frac{1}{(1+2B)^{(1+2B)/(2+3B)}} \cdot 2^{1-\alpha}. \tag{20.142}$$

Equation (20.133), when applied to the adiabats numerically computed by Vardya [Va60a], yields results which agree to 3 or 4 significant figures with Vardya's results.